CENP-C stabilizes the conformation of CENP-A nucleosomes within the inner kinetochore

at human centromeres

Daniël P. Melters[1,*], Tatini Rakshit[1,*], Sergei A. Grigoryev[2], David Sturgill[1], and Yamini Dalal[1,#]

1 National Cancer Institute, Center for Cancer Research, Laboratory of Receptor Biology and Gene Expression, Bethesda, MD

2 Pennsylvania State University, College of Medicine, Hershey, PA

* Contributed equally

Corresponding author: dalaly@mail.nih.gov

Keyword: chromosome, mitosis, kinetochore, nucleosomes, chromatin, centromere

Abstract

The centromere is a vital locus on each chromosome which seeds the kinetochore, allowing for a physical connection between the chromosome and the mitotic spindle. At the heart of the centromere is the centromere-specific histone H3 variant CENP-A/CENH3. Throughout the cell cycle the constitutive centromere associated network is bound to CENP-A chromatin, but how this protein network modifies CENP-A nucleosome dynamics *in vivo* is unknown. Here, using a combination of biophysical and biochemical analyses we provide evidence for the existence of

two populations of structurally distinct CENP-A nucleosomes that co-exist at human centromeres. These two populations display unique sedimentation patterns, which permits purification of inner kinetochore bound CENP-A chromatin away from bulk CENP-A nucleosomes. The bulk population of CENP-A nucleosomes have diminished heights and weakened DNA interactions, whereas CENP-A nucleosomes robustly associated with the inner kinetochore are stabilized in an octameric conformation, with restricted access to nucleosomal DNA. Immuno-labeling coupled to atomic force microscopy of these complexes confirms their identity at the nanoscale resolution. These data provide a systematic and detailed description of inner-kinetochore bound CENP-A chromatin from human centromeres, with implications for the state of CENP-A chromatin that is actively engaged during mitosis.

Introduction

The kinetochore is a large proteinaceous complex which physically connects centromeric chromatin to the mitotic microtubule spindles. Inaccuracies in kinetochore assembly can lead to the formation of dicentric chromosomes, or chromosomes lacking kinetochores. In either case, chromosomes fail to segregate faithfully, which drives genomic instability. Electron microscopy studies of mitotic centromeres reveal a two-layered electron dense structure that is over 200 nm in width and over 50 nm in depth (1–4), delineated into the inner and outer kinetochore.

At the base of the inner kinetochore is the histone H3 variant CENP-A (CENH3), which is marked by its rapid evolution (5–10), and its association with equally rapid evolving centromere DNA (11). This enhanced rate of evolution of sequences underlying the essential and conserved function is commonly referred to as the centromere paradox (12). Nevertheless, despite lack of

sequence conservation at the level of CENP-A, and its associated DNA, in most species, CENP-A chromatin provides the epigenetic and structural foundation to assemble the kinetochore, recruiting inner kinetochore proteins CENP-B, CENP-N, and CENP-C (13, 14). Together, these inner kinetochore components provide recognition motifs for outer kinetochore proteins in the conserved KMN network (KLN1, MIS12 and NDC80 complexes (15–18). Deleting either CENP-A or CENP-C results in cell death or senescence (19–21), but this happens only after a few cell cycles. These data indicate that both CENP-A and CENP-C are often present in excess for what is required to form a functional kinetochore for one cell cycle. Furthermore, CENP-A and CENP-C are long lived proteins guaranteeing faithful chromosome segregation even after their respective genes have been deleted (22–26).

Despite major advances made in understanding the hierarchy of the centromere and kinetochore proteins (21, 27–29), little is known about the physical features of the inner kinetochore bound to centromeric chromatin in higher eukaryotes. Individual mitotic kinetochores were isolated from budding yeast by using a FLAG-tagged outer kinetochore component Dsn1 as bait (30). Point centromeres of budding yeast are unique because they display a one-to-one correspondence, in which a single CENP-A containing nucleosome residing on a 120bp fragment of unique DNA (31–38) binds to a single microtubule via the kinetochore. In contrast, the human centromeres are regional centromeres comprised of megabase-sized α-satellite arrays (39, 40). Recent advances in super resolution microscopy suggest that each human centromere harbors ~400 CENP-A molecules (41), which eventually associate with only ~17 mitotic microtubule spindles (42). This inner kinetochore chromatin is thought to be folded into a boustrophedon (43, 44), in which the number of CENP-A nucleosomes present appears to exceed the number needed for centromere

function. Thus, in order to uncover physical properties that define the regional centromere, it is of interest to purify chromatin associated with the inner kinetochore.

In this report, using nanoscale imaging and biochemical approaches, we provide the first systematic dissection of components and properties of centromeric chromatin bound to the inner kinetochore complex purified from human cells. We report that two distinctive classes of CENP-A nucleosomes co-exist in human cells. One class of CENP-A nucleosomes is weakly associated with inner kinetochore proteins, sediments in the lighter fractions of sucrose gradients, has weaker associations with nucleosome DNA, and possesses diminutive dimensions; whereas a second class of CENP-A nucleosomes co-elute and co-purify with inner kinetochore proteins, have highly stable interactions with DNA, and display octameric dimensions. Both classes of nucleosome are present on alpha-satellite centromeric repeats deriving from the centromere. These data support a model in which, *in vivo,* a pool of CENP-A particles exist in nucleosomes that wrap DNA loosely, whereas an active inner kinetochore complex contains stabilized CENP-A nucleosomes.

Material and Methods

Key Resources Table

Reagents or Resource	Source	Identifier	Application	Quantity
ACA serum	BBI Solutions	SG140-2	N-ChIP, X-ChIP	5 μL
Anti-CENP-A (rabbit)	Abcam	ab45694	WB	1:3000
Anti-CENP-A (rabbit)	Milipore	04-205	WB	1:3000
Anti-CENP-B (rabbit)	Santa Cruz	sc-22788	WB	1:500
Anti-CENP-C (guinea pig)	MBL International	PD030	N-ChIP, X-ChIP	5 μL
Anti-CENP-C (rabbit)	Santa Cruz	sc-22789	WB	1:500
Anti-CENP-N	Avivasysbio	ARP57258-P050	WB	1:500
Anti-CENP-I	Bethyl	A303-374A	WB	1:1000
Anti-CENP-T	Bethyl	A302-314A	WB	1:1000
Anti-CENP-W	Invitrogen	PA5-34441	WB	1:300

Anti-MIS12	Abcam	ab70843	WB	1:500
Anti-HEC1/NDC80	GeneTex	GTX70268	WB	1:1000
Anti-macroH2A.1	Abcam	ab37264	WB	1:1000
Anti-γH2A.X	Abcam	ab2893	WB	1:1000
Anti-H2A.Z	Abcam	ab4179	WB	1:1000
Anti-H2A	Abcam	ab18255	WB	1:1000
Anti-H2B	Abcam	ab1790	WB	1:1000
Anti-H4	Cell Signaling	2935T	WB	1:1000
Anti-H3	Santa Cruz	sc-8654	WB	1:3000

Software and Algorithms		
RepBase		hhtp://www.girinst.org/repbase
Gwyddion		http://gwyddion.net/
R		https://www.r-project.org/
NIH ImageJ		https://imagej.nih.gov/ij/
Bio-Formats		https://www.openmicroscopy.org/bio-formats/

Native and cross-linked Chromatin-Immunoprecipitation and western blotting

Human cell line HeLa were grown in DMEM (Invitrogen/ThermoFisher Cat #11965) supplemented with 10% FBS and 1X penicillin and streptomycin cocktail. N-ChIP experiments were performed without fixation. After cells were grown to ~80% confluency, they were harvested as described (45, 46). For best results for chromatin preparation for AFM the pellet that is obtained after each spin-down during the nuclei extraction protocol (47) is broken up with a single gentle tap. Nuclei were digested for 6 minutes with 0.25 U MNase/mL (Sigma-Aldrich cat #N3755-500UN) and supplemented with 1.5 mM CaCl$_2$. Following quenching (10 mM EGTA), nuclei pellets were spun down, and chromatin was extracted gently, overnight in an end-over-end rotator, in low salt solution (0.5X PBS; 0.1 mM EGTA; protease inhibitor cocktail (Roche cat #05056489001). N-ChIP chromatin bound to Protein G Sepharose beads (GE Healthcare cat #17-0618-02) were gently washed twice with ice cold 0.5X PBS and spun down for 1 minute at 4ºC at 800 rpm. Following the first N-ChIP, the unbound fraction was used for

5

the sequential N-ChIP. X-ChIP experiments were performed with fixation (48). Westerns analyses were done using LiCor's Odyssey CLx scanner and Image Studio v2.0.

Glycerol gradient sedimentation

A total of 2 mL of extracted chromatin was applied to 10 mL of 5 to 20% glycerol gradient containing 50 mM Tris-HCl pH 8.0, 2 mM EDTA, 0.1% NP-40, 2 mM DTT, 0.15 M NaCl, and 1X protease inhibitor cocktail layered over 0.4 mL of 50% glycerol. The chromatin was centrifuged with a SW41Ti rotor (Beckman) at 22,000 rpm for 15.5 hours at 4ºC. 1 mL aliquots were fractioned from the top, and DNA and protein samples were separated by either 1.2% agarose gel electrophoreses or 4-20% SDS-PAGE gels, respectively. Serial N-ChIP was performed on all 12 fractions.

AFM and image analysis

Imaging of CENP-C and CENP-A N-ChIP and bulk chromatin was performed as described (47, 49) with the following modifications. Imaging was performed by using standard AFM equipment (Oxford Instruments, Asylum Research's Cypher S AFM, Santa Barbara, CA) with silicon cantilevers (OTESPA or OTESPA-R3 with nominal resonances of ~300 kHz, stiffness of ~42 N/m, and tip radii of 3–7 nm) in noncontact tapping mode. 10 µl of bulk , CENP-A, or CENP-C chromatin sample was deposited on APS-treated mica (47, 49). The samples were incubated for 10 min, rinsed gently to remove salts, and dried mildly under vacuum before imaging. Automated image analysis was performed as described in (47) with the only modifications that R software was used instead of Microsoft Excel. A total of six biological replicates were performed for CENP-C experiments and three biological replicates for both the CENP-A and bulk

6

chromatin experiments. Bulk chromatin from the same preparation was imaged in parallel to get the baseline octameric range. For all samples, manual spot analyses were performed to confirm accuracy of automated analyses.

Immuno-AFM

In vitro reconstitution of CENP-A (CENP-A/H4 cat#16-010 and H2A/H2B cat#15-0311, EpiCypher, Research Triangle Park, NC) and H3 (H3/H4 cat#16-0008 and H2A/H2B cat#15-0311, EpiCypher Research Triangle Park, NC) nucleosomes were performed as previously described (47, 49). Chromatin from HeLa cells were obtained from fractions 6 and 7 of a glycerol density gradient (containing on average tri-, tetra-, and penta-nucleosome arrays). These samples were subjected to immuno-AFM as described previously (50–52). An aliquot of each sample was imaged by AFM in non-contact tapping mode. The remainder of the samples were incubated overnight at 4ºC with anti-CENP-A antibody (Abcam cat #ab13939) in an end-over-end rotator before being imaged by AFM. Finally, these samples were incubated with anti-mouse secondary antibody (Li-Cor's IRDye 800CW Donkey anti-mouse IgG cat#925-32212) for an hour at room-temperature in an end-over-end rotator and imaged by AFM in non-contact tapping mode. We analyzed the height profiles of the nucleosomes and antibody complexes as described above.

Transmission electron microscopy

For transmission electron microscopy (TEM), the N-ChIP samples were fixed by adding 0.1% glutaraldehyde at 4ºC for 5 hours, followed by 12-hour dialysis against HNE buffer (10 mM HEPES pH=7.0, 5 mM NaCl, 0.1 mM EDTA) in 20,000 MWCO membranes dialysis cassettes

(Slide-A-Lyzer Dialysis Cassette, ThermoFisher cat #66005) at 4ºC. The dialyzed samples were diluted to about 1 μg/mL concentration with 67.5 mM NaCl, applied to carbon-coated and glow-discharged EM grids (T1000-Cu, Electron Microscopy Sciences), and stained with 0.04% uranyl acetate. Dark-field EM imaging was conducted at 120 kV using JEM-1000 electron microscope (JEOL USA, Peabody, MA) with SC1000 ORIUS 11 megapixel CCD camera (Gatan, Inc. Warrendale, PA).

ChIP-ExoIII/MNase

Chromatin (digested for 15 min to obtain mostly mononucleosomes) was obtained by serial N-ChIP and the unbound fraction represented bulk chromatin. ChIP-exo was performed as described in (53, 54) with the following modifications. Chromatin was warmed to 30ºC and digested with 0.25 units MNase and 20 units ExoIII for 3 minutes at 30ºC. The digestion was stopped by adding 20 μL 50 mM EDTA and 5% SDS. Subsequently, proteinase K was added to the samples for 1 hours and DNA was extracted by phenol/chloroform and phenol protocol and ran on a 10% Novex TBE gel (ThermoFisher cat #EC6275BOX). The gel was post-stained with Syto 60 (Invitrogen cat #S11342) and imaged with the LiCor's Odyssey CLx scanner and Image Studio v2.0.

ChIP-DNase I

Chromatin (digested for 15 min to obtain mostly mononucleosomes) was obtained by serial N-ChIP and the unbound fraction represents bulk chromatin. ChIP-DNase I was performed as described in (55) with the following modifications. Chromatin was chilled on ice and digested with 50 U of DNase I on ice for 50 minutes. The reaction was stopped by adding 20 mM EDTA

and 5% SDS, followed by proteinase K. DNA was extracted by phenol/phenol chloroform

extraction and ran on a 10% Novex TBE + urea gel (Invitrogen cat #EC6875BOX). The gel was

post-stained with Syto 60 (Invitrogen cat #S11342) and imaged with the LiCor's Odyssey CLx

scanner and Image Studio v2.0.

ChIP-seq

CENP-C N-ChIP followed by ACA N-ChIP was conducted, as well as an IgG N-ChIP and input

control as described above. Next, DNA was isolated by first proteinase K treated the samples,

followed by DNA extraction by phenol chloroform. The samples were used to prepare libraries

for PacBio single-molecule sequencing as described in manufacturer's protocol (PacBio, Menlo

Park, CA). Libraries were produced and loaded on ZWM chip either by diffusion or following

size selection of the inserts (> 1000 bp) for all four samples. Subsequently, the reads were

sequenced on the PacBio RS II operated by Advanced Technology Center, NCI (Frederick, MD).

Sequence reads were mapped to either sequences in RepBase, the consensus sequence used by

Hasson et al 2013 (56), and the consensus sequences used by Henikoff et al 2015 (57).

Results

CENP-C-associated CENP-A chromatin sediments differently from bulk CENP-A

chromatin

In previous work, we purified human CENP-A nucleosomes under a range of conditions, and

analyzed them by various biochemical, EM and AFM approaches (45, 49). We occasionally

noticed a small fraction of macromolecular complexes within CENP-A native chromatin-

immunoprecipitation (N-ChIP), that were large, compacted, and refractory to standard

9

nucleosome analysis (45, 49). We were curious to examine whether such larger complexes might represent the intact inner kinetochore complex.

Therefore, we developed a gentle, native, serial chromatin-immunoprecipitation assay to purify CENP-C bound chromatin from HeLa cells (Figure 1A, Supplemental Figure S1). We mildly digested nuclear chromatin with micrococcal nuclease (MNase), and then size-separated the extracted chromatin on a glycerol gradient (Figure 1B). This protocol resulted in a mixture of nucleosome arrays (fractions 2-12). A Coomassie stain confirmed that these fractions contained histones (Figure 1C). From these samples, we performed our N-ChIP to first pulled-down CENP-C bound chromatin (Figure 1D) and subsequently pull-down any remaining CENP-A chromatin using ACA serum (58) (Figure 1E).

By Western blot analysis, we observed that both the first CENP-C N-ChIP and the subsequent ACA N-ChIP pulled-down CENP-A chromatin (Figure 1D, E), albeit with different sedimentation patterns (Figure 1D-F). The relative abundance of longer chromatin arrays in the CENP-C N-ChIP was also observed by high resolution capillary electrophoresis (BioAnalyzer, Supplemental Figure S2). These data suggest that two separable populations of native CENP-A may co-exist *in vivo*.

A sub-fraction of CENP-A nucleosomes associate with inner kinetochore

Next, we used quantitative immunoblotting following serial N-ChIP to quantify the relative abundance of native CENP-A bound to CENP-C (Figure 2A). The enrichment of the N-ChIP'ed sample was measured over the input (Figure 2B). CENP-A was enriched 4.4-fold (SE 0.9) in the

CENP-C N-ChIP, whereas CENP-A was enriched 28.5-fold (SE 6.9) in the serial ACA N-ChIP (Figure 2C; Supplemental Table S1). Thus, our results indicate that in HeLa cells, there is a ~6-fold excess of CENP-A that is not strongly associated with CENP-C.

To test the possibility that during the experimental procedure of N-ChIP, CENP-C dissociates from CENP-A chromatin, we also cross-linked samples prior to ChIP. Although in our hands overall chromatin extraction efficiency is generally lower under X-ChIP conditions, the relative pull-down quantities of either CENP-C-associated CENP-A and bulk CENP-A was comparable (Figure 2D-F, Supplemental Table S1). These data support the observation that there is a sizeable fraction of CENP-A chromatin which is not strongly associated with CENP-C, and a smaller fraction of CENP-A that is robustly bound to CENP-C. We sought to further characterize this latter fraction.

CENP-A nucleosomes bound to CENP-C also associate with CCAN kinetochore components

The chromatin we extracted came from cycling HeLa cells (Figure 3A), the majority of which are in G1 phase (59). Throughout the cell cycle the constitutive centromere associated network (CCAN) complex, which is composed of several proteins, is bound to the centromeric chromatin to form the inner kinetochore (Figure 3A) (21, 60). To test whether other components of the CCAN are present within the complex within CENP-A:CENP-C above, we performed western blot analyses on these purified CENP-C complexes. In addition to CENP-A, H2A, and H2B, CCAN components CENP-B, CENP-I, CENP-N, CENP-W, and CENP-T were enriched (Figure 3B). To our surprise, the dedicated chaperone for CENP-A assembly, HJURP was enriched in

the CENP-C N-ChIP. The latter data are consistent with a recent report from bioID experiments that HJURP is associated with CENP-A chromatin at multiple points of the cell cycle (61). Overall, our purified CENP-A:CENP-C complex robustly represents the CCAN components. Furthermore, outer kinetochore components MIS12 and HEC1/NDC80 were also enriched in the CENP-C N-ChIP (Figure 3B). Altogether, from these data, we deduced that the large CENP-C complex that was enriched in fraction 12 of our gradient experiments (Figure 1D) represents the CCAN, and possibly even fully matured kinetochores.

Inner kinetochore associated chromatin is not uniquely enriched in histone H2A variants

We next sought to dissect molecular underpinnings that define the chromatin complex at the inner kinetochore. We considered two specific possibilities: 1) the presence of unique histone variants other than CENP-A; or 2) alterations in the manner in which DNA associates either CENP-A population.

We first interrogated the possibility that CENP-A nucleosomes associated with the inner kinetochore contained other histone variants. Although heterotypic CENP-A/H3.3 nucleosomes have been reported, they are generally restricted to ectopic sites (62, 63). Where histones H4 and H2B have few variants, there are several histone H2A variants including macroH2A, H2A.Z, and γH2A.X (64). As before, we performed a CENP-C N-ChIP followed by a serial ACA N-ChIP and tested both samples for histone H2A variants. Interestingly, we detected H2A.Z and macroH2A variants in both CENP-C and ACA N-ChIP (Figure 3C). However, their relative abundance was not quantifiably different between CENP-C bound vs. free CENP-A chromatin

(Figure 3D, Supplemental Table S2). Consequently, these data do not, a priori, provide evidence that H2A variants contribute to structural differences between the two CENP-A populations.

Inner kinetochore associated CENP-A nucleosomes are inaccessible to DNase I

DNA is an equal player in the nucleosome- therefore, a second possibility for molecular constituents differentiating the two CENP-A populations may arise from the DNA bound to each type of complex. We next examined whether DNA sequence, DNA accessibility, or DNA wrapping is altered in either CENP-A population.

We first tested whether DNA sequence composition might contribute to the two populations of CENP-A. To this end, we performed N-ChIP-seq coupled to PacBio sequencing for both CENP-C N-ChIP and bulk CENP-A N-ChIP. Indeed, these data suggest both CENP-A populations reside on similar centromeric alpha-satellite DNA sequences (Supplemental Figure S3).

We next tested whether the nucleosomal DNA core/linker junctions were equally accessible in both populations. To do this, we used a combination of Exonuclease III and Micrococcal nuclease, which digests in from the linker DNA and pauses at the core-to-linker junction (53). Whether CENP-A nucleosomes were associated with CENP-C or not, the ends of nucleosomal DNA were equally accessible (Figure 4A). Interestingly, in both cases, CENP-A nucleosomes were markedly more accessible compared to H3 nucleosomes (Figure 4A). These data suggest that in the presence of CENP-C *in vivo*, CENP-A nucleosomal DNA does not alter its exit/entry accessibility.

Canonical H3 Nucleosomes wrap 147 bp, but CENP-A nucleosomes only wrap 120 bp (65). To assess how accessible the DNA wrapped around nucleosomes are, we turned to the classical DNase I assay. DNase I creates double strand breaks by cutting only at the minor groove of the DNA double helix. When DNA is wrapped around a nucleosome core particle, the minor groove is only exposed every 10-bp (66, 67). Indeed, this method was first used in a seminal paper 45 year ago (66) to demonstrate that 147-bp DNA is wrapped outside and around the octameric H3 nucleosome core.

When native H3 nucleosomes were digested with DNase I and resolved on high resolution Urea PAGE gels, as expected, a ~10-bp ladder going up to 140-bp was observed (Figure 4B, C). In contrast, bulk CENP-A nucleosomes displayed larger periodicity without a clear 10-bp ladder, potentially indicative of overwound DNA. To our surprise, CENP-C-associated CENP-A nucleosomes displayed a strikingly refractory nature for DNase I digestion (Figure 4B, C), where the nuclease seems unable to clip the CENP-A nucleosome in the presence of CENP-C. These digestion patterns suggest that while DNA ends are equally accessible for both CENP-A populations, bulk CENP-A nucleosomes wrap DNA loosely, whereas the inner kinetochore imposes a physical impassivity onto the CENP-A nucleosome.

Immuno-AFM confirms presence of CENP-A nucleosomes associated with the CENP-C complex

We next turned to visual analysis of these purified inner kinetochore chromatin structures. First, we wanted to confirm the identity of nucleosomes associated with CENP-C using an independent visual approach that is complementary to the Western blot analyses provided above (Figures 1-

14

2). To do this, we developed a single-molecule based method to test whether CENP-A nucleosomes are physically present in CENP-C N-ChIP samples. Inspired by classical immuno-EM protocols and recognition-AFM (68), in which one can confirm the identity of a given molecule in a biological sample, we adapted immuno-labeling for in-air atomic force microscopy (AFM) (Figure 5A). We first visualized either without antibody; or, 1º mouse monoclonal anti-CENP-A antibody; or, 1º CENP-A antibody and, either 2º anti-mouse antibody or 2º anti-mouse Fab fragment. The 1º antibody by itself was 0.8±0.2 nm in height and the addition of the 2º antibody resulted in a height increase to 2.0±0.5 nm (Figure 5B, C, Supplemental Table S3, Raw Data File 1). To confirm the 1º antibody's specificity, we *in vitro* reconstituted recombinant H3 or CENP-A nucleosomes as before, and incubated them with either no antibody (no Ab); primary antibody (1º); or, primary plus secondary (2º) antibodies respectively (Figure 5B, C). Whereas *in vitro* reconstituted H3 nucleosomes did not show a shift in particle height in the presence of anti-CENP-A antibodies (no Ab: 2.2±0.2nm, 1º: 2.1±0.2 nm, and 2º: 2.2±0.1 nm, resp.). As expected, these *in vitro* reconstituted CENP-A nucleosomes did increase in height (no Ab: 2.2±0.2 nm, 1º: 2.5±0.3 nm, and 4.6±1.4 nm with 2º antibody, or 3.2±0.6 nm with Fab fragment, resp., Figure 5B, C, S4, Supplemental Table S3, Raw Data File 1).

Next, we applied the same method to native H3 or CENP-C purified complexes (Figure 5B, C). Similar to reconstituted H3 nucleosomes, bulk H3 chromatin did not demonstrate a shift in particle height when incubated with anti-CENP-A antibodies (no Ab: 2.3±0.2 nm, 1º: 2.4±0.3 nm, and 2º: 2.3±0.1 nm, resp.). In contrast, nucleosomal particles that came down in the CENP-C N-ChIP displayed a shift in height when challenged with anti-CENP-A antibodies (no Ab:

2.4±0.4 nm, 1°: 2.6±0.4 nm, and 2°: 3.9±1.3 nm, resp.). These results support the biochemical interpretation that CENP-A nucleosomes are associated with the purified CENP-C complex.

Physically taller CENP-A nucleosomes are bound to the inner kinetochore

We next examined the physical characteristics of this inner kinetochore associated CENP-A chromatin. In order to image these complexes, we split the samples in half, and imaged the same samples independently using two high resolution single-molecule methods: in-air AFM; and transmission electron microscopy (TEM) (Figure 6A, B, S5). By AFM and TEM, we observed large polygonal structures with a roughly circular footprint (height: 5.8±2.1 nm; area: 629±358 nm^2) associated with four to six nucleosomes (Figure 6A, B, S5, Table S4, Raw Data File 2). Compared to individual nucleosomes, these complexes were substantially larger. These structures were not observed in either mock IP, bulk chromatin, or CENP-A N-ChIP (Figure 5A, B, S5), suggesting specificity arising from CENP-C bound complexes. Additionally, the largest of CENP-C complexes was associated with a 233±267 bp long nucleosome-free DNA (Figure 6A, Table S4, Raw Data File 2). The same samples, analyzed in parallel by TEM, displayed similar features (Figure 6B), including the association of four to six nucleosomes at the periphery of the CENP-C complex.

We next turned our attention to the nucleosomes associated with CENP-C. In our previous work, recombinant octameric CENP-A nucleosomes on 601 or α-satellite DNA behave similar to H3 when measured by in-air AFM, with average heights of ~2.4 nm and widths of ~12 nm (62, 69). This observation is consistent with static measurements made by biophysical, EM, and crystallographic methods, which generally show that except for flexible exit/entry DNA termini

16

and loop 1, *in vitro* reconstituted CENP-A nucleosomes have dimensions similar to H3 nucleosomes (63, 65, 69–71).

In contrast, native CENP-A nucleosomes purified from either fruit fly or human cell lines display smaller dimensions compared to native H3 nucleosomes, except during S phase (45, 49, 62, 72, 73). Indeed, we recapitulated these observations here. Relative to H3 nucleosomes (2.5±0.3 nm) (Figure 6C, Table S5, Raw Data File 3), native bulk CENP-A nucleosomes not associated with CENP-C, and are uniquely identifiable by a smaller average height of 1.9±0.3 nm (Figure 6C).

We next examined CENP-A nucleosomes that are physically present within CENP-C complexes (Figure 6C, Table S5, Raw Data File 3). To our surprise, these nucleosomes had distinct octameric dimensions, with a height of 2.4±0.5 nm (Figure 6C), significantly taller than bulk CENP-A nucleosomes alone (two-sided t-test p < 0.001).

These results point to the presence of two physically distinct CENP-A nucleosomes within the human centromere: one species of CENP-A nucleosome which is shorter, and another species of CENP-A nucleosome, which is associated with the CENP-C complex (Figure 6D), and which adopts a conformation similar to that of H3 nucleosomes.

Discussion

Since the discovery of CENP-A (58, 74), it has been demonstrated that CENP-A nucleosomes are required and sufficient to form kinetochores (13, 14). At the same time, it is puzzling that more CENP-A nucleosomes reside at the centromere than are strictly needed to successfully seed

17

a kinetochore (21, 25). Indeed, a recent chromatin fiber study which employed a proximity based labeling technique, provided important clues that not all CENP-A foci colocalize with CENP-C foci (75). Here, our data supports, and extends this case. We report on the existence of two structurally distinct populations of CENP-A nucleosomes *in vivo*. One population of CENP-A nucleosomes was strongly associated with the CENP-C complex, along with other components of the inner kinetochore; whereas another population of CENP-A nucleosomes is weakly, or not associated with CENP-C. Strikingly CENP-A nucleosomes associated with the CENP-C complex were taller than bulk CENP-A nucleosomes (Figure 5D). All atom computational modeling has previously indicated that CENP-A nucleosomes have a weaker four helix bundle resulting in an intrinsically more disordered nucleosome core compared to a canonical H3 nucleosome (76), and that this flexibility is seen even in CENP-A/H4 dimers (77). Subsequently, the free energy landscape predicts the existence of multiple conformational states of CENP-A (76). One hypothesis derived from these modeling experiments is that CENP-A nucleosomes display altered nucleosome conformations, and that kinetochore components such as CENP-C could fix one preferred conformational state. Indeed, previous *in vitro* work has shown that both the central domain and the conserved CENP-C motif make contact with the CENP-A C-terminal tail and H2A acidic patch (78). In hydrogen-deuterium exchange and smFRET experiments of *in vitro* reconstituted CENP-A mononucleosomes, these contacts result in changes in the overall shape of CENP-A nucleosome by bringing the two nucleosome halves closer together and limiting the DNA sliding (79–81). As a result, the CENP-A nucleosome when bound to the central domain of CENP-C has an appearance similar to a canonical H3 nucleosome. Indeed, we observe a shift in nucleosomal height when CENP-A nucleosomes associate with CENP-C

complexes. We interpret this shift to mean that the CENP-C complex stabilizes the octameric conformation of the CENP-A nucleosome *in vivo*.

Interestingly, our ChIP-DNase I analysis supports the explanation that CENP-A nucleosomes *in vivo* are associated with underwound DNA (Figure 4), whereas CENP-C associated CENP-A nucleosomes were remarkably resistant to DNase I digestion (Figure 4B, C), refractory to extensive MNase digestion (Figure S2), but accessible to ExoIII/MNase nuclease (Figure 4A).

We considered three possible explanations for the nuclease digestion results. First, the CENP-C complex might physically limit access of DNase I to the nucleosomal DNA by engulfing the nucleosome around the core. This idea is plausible, because full length CENP-C in humans is 140kDa, about the size of an octamer. Secondly, CENP-C (with or without other kinetochore components) might twist the linker DNA to overwind it around the nucleosome, resulting in physically distorted minor grooves, which is biochemically reflected in limited access to DNase I. Tightening of the DNA might also be induced by chromatin remodelers such as RSF, which has been reported to be active at the centromere (82, 83). Third, based on work from budding yeast point centromeres, it is feasible that DNA is positively supercoiled around CENP-A nucleosomes (33), but only when in association with the CENP-C/kinetochore complex. This is suggested by results from budding yeast, in which the CBF3 complex induces a 70-bp positive supercoiling loop (38), which can be accommodated by both CENP-A and H3 nucleosomes (33, 63). Indeed, our own prior biophysical analyses using magnetic tweezers suggests that both CENP-A and H3 nucleosomes can assemble on pre-assembly positively supercoiled DNA (63). A change in DNA accessibility upon CENP-C binding may also provide the mechanistic

underpinning for the nuclease refractory pattern of yeast centromeres observed by Southern blots in seminal work published three decades ago (31, 32).

In summary, in this report we describe that CENP-A nucleosomes display two alternative conformational states when bound to kinetochore proteins *in vivo*. We note that nucleosome dynamics play an important role in genome compaction, protection from DNA damaging agents, and regulating DNA access by DNA binding complexes. These dynamics are driven by only a few interactions between the interfaces of DNA and nucleosomes (84, 85). Recently, we described a CENP-A core post-translation modification (PTM) that altered the binding with CENP-C *in vivo* (46). An exciting line of future investigation is to examine how DNA or histone modifications spontaneously promote or weaken the free energy landscape of CENP-A nucleosomes, altering its interactions with kinetochore partners, chaperones, and its occupancy on centromere satellite DNA. It will also be of paramount interest to investigate whether nucleosome stabilizing or destabilizing interactions promote or suppress centromeric transcription required for the epigenetic memory of centromeres in various species (86–102), and for chaperone interactions required for correct targeting of CENP-A, which we, and others, have demonstrated is defective in cancer cells (62, 77, 103).

Footnotes

Authors contributions: D.P.M. and Y.D. designed research; D.P.M., T.R, S.A.G., and D.S. performed research; D.P.M., T.R. (immuno-AFM), S.A.G. (TEM), D.S. (sequence analysis), and Y.D. analyzed data; D.P.M. prepared figures; and D.P.M. and Y.D. wrote the paper; all authors editing the paper.

The authors declare no conflict of interest.

Acknowledgements

References

1. Comings,D.E. and Okada,T.A. (1970) Whole-mount electron microscopy of the centromere region of metacentric and telocentric mammalian chromosomes. *Cytogenetics*, **9**, 436–49.

2. Rattner,J.B., Branch,A. and Hamkalo,B.A. (1975) Electron microscopy of whole mount metaphase chromosomes. *Chromosoma*, **52**, 329–38.

3. Esponda,P. (1978) Cytochemistry of kinetochores under electron microscopy. *Exp. Cell Res.*, **114**, 247–52.

4. McEwen,B.F., Hsieh,C.E., Mattheyses,A.L. and Rieder,C.L. (1998) A new look at kinetochore structure in vertebrate somatic cells using high-pressure freezing and freeze substitution. *Chromosoma*, **107**, 366–75.

5. Malik,H.S. and Henikoff,S. (2001) Adaptive evolution of Cid, a centromere-specific histone.

Dros. Genet., **157**, 1293–1298.

6. Malik,H.S. and Henikoff,S. (2003) Phylogenomics of the nucleosome. *Nat. Struct. Biol*, **10**, 882–891.

7. Talbert,P.B., Bryson,T.D. and Henikoff,S. (2004) of Biology BioMed Central Adaptive evolution of centromere proteins in plants and animals. *J. Biol.*

8. Cooper,J.L. and Henikoff,S. (2004) Adaptive evolution of the histone fold domain in centromeric histones. *Mol. Biol. Evol*, **21**, 1712–1718.

9. Meraldi,P., Mcainsh,A.D., Rheinbay,E. and Sorger,P.K. (2006) Phylogenetic and structural analysis of centromeric DNA and kinetochore proteins. *Genome Biol. 7, R23*.

10. Maheshwari,S., Tan,E.H., West,A., Franklin,F.C.H., Comai,L. and Chan,S.W.L. (2015) Naturally Occurring Differences in CENH3 Affect Chromosome Segregation in Zygotic Mitosis of Hybrids. *PLoS Genet.*, 10.1371/journal.pgen.1004970.

11. Melters,D.P., Bradnam,K.R., Young,H.A., Telis,N., May,M.R., Ruby,J.G., Sebra,R., Peluso,P., Eid,J., Rank,D., *et al.* (2013) Comparative analysis of tandem repeats from hundreds of species reveals unique insights into centromere evolution. *Genome Biol.*, **14**.

12. Web,S., Web,I.S.I., Press,H., Biology,M., York,N. and Nw,A. (2009) The Centromere Paradox : Stable Inheritance with Rapidly Evolving DNA. *Science (80-.).*, **1098**.

13. Regnier,V., Vagnarelli,P., Fukagawa,T., Zerjal,T., Burns,E., Trouche,D., Earnshaw,W. and Brown,W. (2005) CENP-A Is Required for Accurate Chromosome Segregation and Sustained Kinetochore Association of BubR1. *Mol. Cell. Biol.*, 10.1128/mcb.25.10.3967-3981.2005.

14. Mendiburo,M.J., Padeken,J., Fülöp,S., Schepers,A. and Heun,P. (2011) Drosophila CENH3 is sufficient for centromere formation. *Science (80-.).*, 10.1126/science.1206880.

15. Cheeseman,I.M., Chappie,J.S., Wilson-Kubalek,E.M. and Desai,A. (2006) The Conserved KMN Network Constitutes the Core Microtubule-Binding Site of the Kinetochore. *Cell*, 10.1016/j.cell.2006.09.039.

16. Przewloka,M.R., Zhang,W., Costa,P., Archambault,V., D'Avino,P.P., Lilley,K.S., Laue,E.D., McAinsh,A.D. and Glover,D.M. (2007) Molecular analysis of core kinetochore composition and assembly in Drosophila melanogaster. *PLoS One*, 10.1371/journal.pone.0000478.

17. DeLuca,J.G. and Musacchio,A. (2012) Structural organization of the kinetochore-microtubule interface. *Curr. Opin. Cell Biol.*, 10.1016/j.ceb.2011.11.003.

18. Weir,J.R., Faesen,A.C., Klare,K., Petrovic,A., Basilico,F., Fischböck,J., Pentakota,S., Keller,J., Pesenti,M.E., Pan,D., *et al.* (2016) Insights from biochemical reconstitution into the architecture of human kinetochores. *Nature*, 10.1038/nature19333.

19. Fukagawa,T., Pendon,C., Morris,J. and Brown,W. (1999) CENP-C is necessary but not sufficient to induce formation of a functional centromere. *EMBO J.*, 10.1093/emboj/18.15.4196.

20. Kwon,M.-S., Hori,T., Okada,M. and Fukagawa,T. (2007) CENP-C Is Involved in Chromosome Segregation, Mitotic Checkpoint Function, and Kinetochore Assembly. *Mol. Biol. Cell*, 10.1091/mbc.e07-01-0045.

21. McKinley,K.L. and Cheeseman,I.M. (2016) The molecular basis for centromere identity and function. *Nat. Rev. Mol. Cell Biol.*, 10.1038/nrm.2015.5.

22. Kalitsis,P., Fowler,K.J., Earle,E., Hill,J. and Choo,K.H.A. (2002) Targeted disruption of mouse centromere protein C gene leads to mitotic disarray and early embryo death. *Proc. Natl. Acad. Sci.*, 10.1073/pnas.95.3.1136.

23. Howman,E. V, Fowler,K.J., Newson,A.J., Redward,S., Macdonald,A.C., Kalitsis,P. and

bioRxiv preprint doi: https://doi.org/10.1101/604223; this version posted April 10, 2019. The copyright holder for this preprint (which was not certified by peer review) is the author/funder. This article is a US Government work. It is not subject to copyright under 17 USC 105 and is also made available for use under a CC0 license.

Choo,K.H.A. (1999) Early disruption of centromeric chromatin organization in centromere protein A (Cenpa) null mice. *Cycle*.

24. Suzuki,A., Hori,T., Nishino,T., Usukura,J., Miyagi,A., Morikawa,K. and Fukagawa,T. (2011) Spindle microtubules generate tension-dependent changes in the distribution of inner kinetochore proteins. *J. Cell Biol.*, 10.1083/jcb.201012050.

25. Bodor,D.L., Valente,L.P., Mata,J.F., Black,B.E. and Jansen,L.E.T. (2013) Assembly in G1 phase and long-term stability are unique intrinsic features of CENP-A nucleosomes. *Mol. Biol. Cell*, 10.1091/mbc.e13-01-0034.

26. Smoak,E.M., Stein,P., Schultz,R.M., Lampson,M.A. and Black,B.E. (2016) Long-Term Retention of CENP-A Nucleosomes in Mammalian Oocytes Underpins Transgenerational Inheritance of Centromere Identity. *Curr. Biol.*, 10.1016/j.cub.2016.02.061.

27. Milks,K.J., Moree,B. and Straight,A.F. (2009) Dissection of CENP-C-directed Centromere and Kinetochore Assembly. *Mol. Biol. Cell*, 10.1091/mbc.e09-05-0378.

28. Cheeseman,I.M. (2014) The Kinetochore. *Cold Spring Harb. Perspect. Biol.*, **6**, a015826–a015826.

29. Klare,K., Weir,J.R., Basilico,F., Zimniak,T., Massimiliano,L., Ludwigs,N., Herzog,F. and Musacchio,A. (2015) CENP-C is a blueprint for constitutive centromere-associated network assembly within human kinetochores. *J. Cell Biol.*, 10.1083/jcb.201412028.

30. Gonen,S., Akiyoshi,B., Iadanza,M.G., Shi,D., Duggan,N., Biggins,S. and Gonen,T. (2012) The structure of purified kinetochores reveals multiple microtubule-attachment sites. *Nat. Struct. Mol. Biol.*, 10.1038/nsmb.2358.

31. Bloom,K.S. and Carbon,J. (1982) Yeast centromere DNA is in a unique and highly ordered structure in chromosomes and small circular minichromosomes. *Cell*, 10.1016/0092-

8674(82)90147-7.

32. Saunders,M., Fitzgerald-hayes,H. and Bloom,K. (1988) Chromatin structure of altered yeast centromeres. *Proc. Null. Acud.*

33. Furuyama,T. and Henikoff,S. (2009) Centromeric nucleosomes induce positive supercoils. *Cell*, **138**, 104–113.

34. Kingston,I.J., Yung,J.S.Y. and Singleton,M.R. (2011) Biophysical characterization of the centromere-specific nucleosome from budding yeast. *J. Biol. Chem.*, 10.1074/jbc.M110.189340.

35. Krassovsky,K., Henikoff,J.G. and Henikoff,S. (2011) Tripartite organization of centromeric chromatin in budding yeast. *Proc. Natl. Acad. Sci.*, 10.1073/pnas.1118898109.

36. Furuyama,T., Codomo,C.A. and Henikoff,S. (2013) Reconstitution of hemisomes on budding yeast centromeric DNA. *Nucleic Acids Res.*, 10.1093/nar/gkt314.

37. Henikoff,S., Ramachandran,S., Krassovsky,K., Bryson,T.D., Codomo,C.A., Brogaard,K., Widom,J., Wang,J.-P. and Henikoff,J.G. (2014) The budding yeast Centromere DNA Element II wraps a stable Cse4 hemisome in either orientation in vivo. *Elife*, 10.7554/elife.01861.

38. Díaz-Ingelmo,O., Martínez-García,B., Segura,J., Valdés,A. and Roca,J. (2015) DNA Topology and Global Architecture of Point Centromeres. *Cell Rep.*, 10.1016/j.celrep.2015.09.039.

39. Waye,J.S. and Willard,H.F. (2006) Human beta satellite DNA: genomic organization and sequence definition of a class of highly repetitive tandem DNA. *Proc. Natl. Acad. Sci.*, 10.1073/pnas.86.16.6250.

40. Rudd,M.K., Wray,G.A. and Willard,H.F. (2006) The evolutionary dynamics of α -satellite

The evolutionary dynamics of ␣ -satellite. *Genome Res.*, 10.1101/gr.3810906.

41. Bodor,D.L., Mata,J.F., Sergeev,M., David,A.F., Salimian,K.J., Panchenko,T., Cleveland,D.W., Black,B.E., Shah,J. V and Jansen,L.E. (2014) The quantitative architecture of centromeric chromatin. *Elife*, 10.7554/elife.02137.

42. Suzuki,A., Badger,B.L. and Salmon,E.D. (2015) A quantitative description of Ndc80 complex linkage to human kinetochores. *Nat. Commun.*, 10.1038/ncomms9161.

43. Ribeiro,S.A., Vagnarelli,P., Dong,Y., Hori,T., McEwen,B.F., Fukagawa,T., Flors,C. and Earnshaw,W.C. (2010) A super-resolution map of the vertebrate kinetochore. *Proc. Natl. Acad. Sci.*, 10.1073/pnas.1002325107.

44. Vargiu,G., Makarov,A.A., Allan,J., Fukagawa,T., Booth,D.G. and Earnshaw,W.C. (2017) Stepwise unfolding supports a subunit model for vertebrate kinetochores. *Proc. Natl. Acad. Sci.*, 10.1073/pnas.1614145114.

45. Bui,M., Dimitriadis,E.K., Hoischen,C., An,E., Quénet,D., Giebe,S., Nita-Lazar,A., Diekmann,S. and Dalal,Y. (2012) Cell-cycle-dependent structural transitions in the human CENP-A nucleosome in vivo. *Cell*, 10.1016/j.cell.2012.05.035.

46. Bui,M., Pitman,M., Nuccio,A., Roque,S., Donlin-Asp,P.G., Nita-Lazar,A., Papoian,G.A. and Dalal,Y. (2017) Internal modifications in the CENP-A nucleosome modulate centromeric dynamics. *Epigenetics and Chromatin*, 10.1186/s13072-017-0124-6.

47. Walkiewicz,M.P., Bui,M., Quénet,D. and Dalal,Y. (2014) Tracking histone variant nucleosomes across the human cell cycle using biophysical, biochemical, and cytological analyses. *Methods Mol. Biol.*, 10.1007/978-1-4939-0888-2_34.

48. Skene,P.J. and Henikoff,S. (2015) A simple method for generating highresolution maps of genome-wide protein binding. *Elife*, 10.7554/eLife.09225.

49. Dimitriadis,E.K., Weber,C., Gill,R.K., Diekmann,S. and Dalal,Y. (2010) Tetrameric organization of vertebrate centromeric nucleosomes. *Proc. Natl. Acad. Sci.*, 10.1073/pnas.1009563107.

50. M. E. Browning-Kelley,†, K. Wadu-Mesthrige,‡, V. Hari,*,† and and G. Y. Liu*,‡ (1997) Atomic Force Microscopic Study of Specific Antigen/Antibody Binding. 10.1021/LA960918X.

51. Cheung,J.W.C. and Walker,G.C. (2008) Immuno-Atomic Force Microscopy Characterization of Adsorbed Fibronectin. *Langmuir*, **24**, 13842–13849.

52. Banerjee,S., M,A., Rakshit,T., Roy,N.S., Kundu,T.K., Roy,S. and Mukhopadhyay,R. (2012) Structural features of human histone acetyltransferase p300 and its complex with p53. *FEBS Lett.*, **586**, 3793–3798.

53. Nikitina,T., Wang,D., Gomberg,M., Grigoryev,S.A. and Zhurkin,V.B. (2013) Combined micrococcal nuclease and exonuclease III digestion reveals precise positions of the nucleosome core/linker junctions: Implications for high-resolution nucleosome mapping. *J. Mol. Biol.*, 10.1016/j.jmb.2013.02.026.

54. Cole,H.A., Cui,F., Ocampo,J., Burke,T.L., Nikitina,T., Nagarajavel,V., Kotomura,N., Zhurkin,V.B. and Clark,D.J. (2016) Novel nucleosomal particles containing core histones and linker DNA but no histone H1. *Nucleic Acids Res.*, 10.1093/nar/gkv943.

55. Staynov,D.Z. (2000) DNase I digestion reveals alternating asymmetrical protection of the nucleosome by the higher order chromatin structure. *Nucleic Acids Res.*

56. Hasson,D., Panchenko,T., Salimian,K.J., Salman,M.U., Sekulic,N., Alonso,A., Warburton,P.E. and Black,B.E. (2013) The octamer is the major form of CENP-A nucleosomes at human centromeres. *Nat. Struct. Mol. Biol.*, 10.1038/nsmb.2562.

27

57. Henikoff,J.G., Thakur,J., Kasinathan,S. and Henikoff,S. (2015) A unique chromatin complex occupies young a-satellite arrays of human centromeres. *Sci. Adv.*, 10.1126/sciadv.1400234.

58. Earnshaw,W.C. and Rothfield,N. (1985) Identification of a family of human centromere proteins using autoimmune sera from patients with scleroderma. *Chromosoma*, 10.1007/BF00328227.

59. Pettersen,E.O., Bakke,O., Lindmo,T. and Oftebro,R. (1977) CELL CYCLE CHARACTERISTICS OF SYNCHRONIZED AND ASYNCHRONOUS POPULATIONS OF HUMAN CELLS AND EFFECT OF COOLING OF SELECTED MITOTIC CELLS. *Cell Prolif.*, 10.1111/j.1365-2184.1977.tb00309.x.

60. Pesenti,M.E., Weir,J.R. and Musacchio,A. (2016) Progress in the structural and functional characterization of kinetochores. *Curr. Opin. Struct. Biol.*, 10.1016/j.sbi.2016.03.003.

61. Remnant,L., Booth,D.G., Vargiu,G., Spanos,C., Kerr,A.R.W. and Earnshaw,W.C. (2019) *In vitro* BioID: Mapping the CENP-A Micro-Environment with high temporal and spatial resolution. *Mol. Biol. Cell*, 10.1091/mbc.E18-12-0799.

62. Athwal,R.K., Walkiewicz,M.P., Baek,S., Fu,S., Bui,M., Camps,J., Ried,T., Sung,M.H. and Dalal,Y. (2015) CENP-A nucleosomes localize to transcription factor hotspots and subtelomeric sites in human cancer cells. *Epigenetics and Chromatin*, 10.1186/1756-8935-8-2.

63. Vlijm,R., Kim,S.H., De Zwart,P.L., Dalal,Y. and Dekker,C. (2017) The supercoiling state of DNA determines the handedness of both H3 and CENP-A nucleosomes. *Nanoscale*, 10.1039/c6nr06245h.

64. Melters,D.P., Nye,J., Zhao,H. and Dalal,Y. (2015) Chromatin dynamics in vivo: A game of musical chairs. *Genes (Basel).*, **6**.

65. Tachiwana,H., Kagawa,W., Shiga,T., Osakabe,A., Miya,Y., Saito,K., Hayashi-Takanaka,Y., Oda,T., Sato,M., Park,S.Y., *et al.* (2011) Crystal structure of the human centromeric nucleosome containing CENP-A. *Nature*, 10.1038/nature10258.

66. Noll,M. (1974) Internal structure of the chromatin subunit. *Nucleic Acids Res.*, 10.1093/nar/1.11.1573.

67. Prunell,A. (1998) A topological approach to nucleosome structure and dynamics: The linking number paradox and other issues. *Biophys. J.*, 10.1016/S0006-3495(98)77961-5.

68. Wang,H., Dalal,Y., Henikoff,S. and Lindsay,S. (2008) Single-epitope recognition imaging of native chromatin. *Epigenetics Chromatin*, 10.1186/1756-8935-1-10.

69. Walkiewicz,M.P., Dimitriadis,E.K. and Dalal,Y. (2014) CENP-A octamers do not confer a reduction in nucleosome height by AFM. *Nat. Struct. Mol. Biol.*, **21**, 2–3.

70. Roulland,Y., Ouararhni,K., Naidenov,M., Ramos,L., Shuaib,M., Syed,S.H., Lone,I.N., Boopathi,R., Fontaine,E., Papai,G., *et al.* (2016) The Flexible Ends of CENP-A Nucleosome Are Required for Mitotic Fidelity. *Mol. Cell*, 10.1016/j.molcel.2016.06.023.

71. Kim,S.H., Vlijm,R., Van Der Torre,J., Dalal,Y. and Dekker,C. (2016) CENP-A and H3 nucleosomes display a similar stability to force-mediated disassembly. *PLoS One*, 10.1371/journal.pone.0165078.

72. Dalal,Y., Wang,H., Lindsay,S. and Henikoff,S. (2007) Tetrameric structure of centromeric nucleosomes in interphase Drosophila cells. *PLoS Biol. 5 e218*.

73. Bui,M., Walkiewicz,M.P., Dimitriadis,E.K. and Dalal,Y. (2013) The CENP-A nucleosome. A battle between Dr. Jekyll and Mr. Hyde. *Nucl. (United States)*, 10.4161/nucl.23588.

74. Palmer,D.K., O'Day,K., Trong,H.L., Charbonneau,H. and Margolis,R.L. (1991) Purification of the centromere-specific protein CENP-A and demonstration that it is a distinctive

histone. *Proc. Natl. Acad. Sci. U. S. A.*

75. Kyriacou,E. and Heun,P. (2018) High-resolution mapping of centromeric protein association using APEX-chromatin fibers. *Epigenetics Chromatin*, **11**, 68.

76. Winogradoff,D., Zhao,H., Dalal,Y. and Papoian,G.A. (2015) Shearing of the CENP-A dimerization interface mediates plasticity in the octameric centromeric nucleosome. *Sci. Rep.*, 10.1038/srep17038.

77. Zhao,H., Winogradoff,D., Bui,M., Dalal,Y. and Papoian,G.A. (2016) Promiscuous Histone Mis-Assembly Is Actively Prevented by Chaperones. *J. Am. Chem. Soc.*, 10.1021/jacs.6b05355.

78. Kato,H., Jiang,J., Zhou,B.R., Rozendaal,M., Feng,H., Ghirlando,R., Xiao,T.S., Straight,A.F. and Bai,Y. (2013) A conserved mechanism for centromeric nucleosome recognition by centromere protein CENP-C. *Science (80-.).*, 10.1126/science.1235532.

79. Falk,S.J., Guo,L.Y., Sekulic,N., Smoak,E.M., Mani,T., Logsdon,G.A., Gupta,K., Jansen,L.E.T., Van Duyne,G.D., Vinogradov,S.A., *et al.* (2015) CENP-C reshapes and stabilizes CENP-A nucleosomes at the centromere. *Science (80-.).*, 10.1126/science.1259308.

80. Falk,S.J., Lee,J., Sekulic,N., Sennett,M.A., Lee,T.H. and Black,B.E. (2016) CENP-C directs a structural transition of CENP-A nucleosomes mainly through sliding of DNA gyres. *Nat. Struct. Mol. Biol.*, 10.1038/nsmb.3175.

81. Guo,L.Y., Allu,P.K., Zandarashvili,L., McKinley,K.L., Sekulic,N., Dawicki-McKenna,J.M., Fachinetti,D., Logsdon,G.A., Jamiolkowski,R.M., Cleveland,D.W., *et al.* (2017) Centromeres are maintained by fastening CENP-A to DNA and directing an arginine anchor-dependent nucleosome transition. *Nat. Commun.*, 10.1038/ncomms15775.

82. Perpelescu,M., Nozaki,N., Obuse,C., Yang,H. and Yoda,K. (2009) Active establishment of centromeric cenp-a chromatin by rsf complex. *J. Cell Biol.*, 10.1083/jcb.200903088.

83. Lee,H.-S., Lin,Z., Chae,S., Yoo,Y.-S., Kim,B.-G., Lee,Y., Johnson,J.L., Kim,Y.-S., Cantley,L.C., Lee,C.-W., *et al.* (2018) The chromatin remodeler RSF1 controls centromeric histone modifications to coordinate chromosome segregation. *Nat. Commun.*, **9**, 3848.

84. Polach,K.J. and Widom,J. (1995) Mechanism of protein access to specific DNA sequences in chromatin: A dynamic equilibrium model for gene regulation. *J. Mol. Biol.*, 10.1006/jmbi.1995.0606.

85. Widom,J. (2002) STRUCTURE, DYNAMICS, AND FUNCTION OF CHROMATIN IN VITRO. *Annu. Rev. Biophys. Biomol. Struct.*, 10.1146/annurev.biophys.27.1.285.

86. Wong,L.H., Brettingham-Moore,K.H., Chan,L., Quach,J.M., Anderson,M.A., Northrop,E.L., Hannan,R., Saffery,R., Shaw,M.L., Williams,E., *et al.* (2007) Centromere RNA is a key component for the assembly of nucleoproteins at the nucleolus and centromere. *Genome Res.*, 10.1101/gr.6022807.

87. Chueh,A.C., Northrop,E.L., Brettingham-moore,K.H., Choo,K.H.A. and Wong,L.H. (2009) LINE Retrotransposon RNA Is an Essential Structural and Functional Epigenetic Component of a Core Neocentromeric Chromatin. *PLoS Genet.*, **5**.

88. Bobkov,G.O.M., Gilbert,N. and Heun,P. (2018) Centromere transcription allows CENP-A to transit from chromatin association to stable incorporation. *J. Cell Biol.*, 10.1083/jcb.201611087.

89. McNulty,S.M., Sullivan,L.L. and Sullivan,B.A. (2017) Human Centromeres Produce Chromosome-Specific and Array-Specific Alpha Satellite Transcripts that Are Complexed with CENP-A and CENP-C. *Dev. Cell*, 10.1016/j.devcel.2017.07.001.

90. Zhu,J., Cheng,K.C.L. and Yuen,K.W.Y. (2018) Histone H3K9 and H4 Acetylations and Transcription Facilitate the Initial CENP-AHCP-3Deposition and de Novo Centromere Establishment in Caenorhabditis elegans Artificial Chromosomes. *Epigenetics and Chromatin*, 10.1186/s13072-018-0185-1.

91. Ling,Y.H. and Yuen,K.W.Y. (2019) Point centromere activity requires an optimal level of centromeric noncoding RNA. *Proc. Natl. Acad. Sci. U. S. A.*, 10.1073/pnas.1821384116.

92. Grenfell,A.W., Heald,R. and Strzelecka,M. (2016) Mitotic noncoding RNA processing promotes kinetochore and spindle assembly in Xenopus. *J. Cell Biol.*, 10.1083/jcb.201604029.

93. Melters,D.P., Pitman,M., Rakshit,T., Bui,M., Dimitriadis,E.K., Papoian,G.A. and Dalal,Y. (2019) The accessibility of human centromeric chromatin is modulated by elastic CENP-A nucleosomes. *bioRxiv*, 10.1101/392787.

94. Lyn Chan,F. and Wong,L.H. (2012) Transcription in the maintenance of centromere chromatin identity. *Nucleic Acids Res.*, 10.1093/nar/gks921.

95. Li,F., Sonbuchner,L., Kyes,S.A., Epp,C. and Deitsch,K.W. (2008) Nuclear non-coding RNAs are transcribed from the centromeres of Plasmodium falciparum and are associated with centromeric chromatin. *J. Biol. Chem.*, 10.1074/jbc.M707344200.

96. Ferri,F., Bouzinba-Segard,H., Velasco,G., Hubé,F. and Francastel,C. (2009) Non-coding murine centromeric transcripts associate with and potentiate Aurora B kinase. *Nucleic Acids Res.*, 10.1093/nar/gkp529.

97. Bergmann,J.H., Rodríguez,M.G., Martins,N.M.C., Kimura,H., Kelly,D.A., Masumoto,H., Larionov,V., Jansen,L.E.T. and Earnshaw,W.C. (2011) Epigenetic engineering shows H3K4me2 is required for HJURP targeting and CENP-A assembly on a synthetic human

kinetochore. *EMBO J.*, 10.1038/emboj.2010.329.

98. Choi,E.S., Strålfors,A., Castillo,A.G., Durand-Dubief,M., Ekwall,K. and Allshire,R.C. (2011) Identification of noncoding transcripts from within CENP-A chromatin at fission yeast centromeres. *J. Biol. Chem.*, 10.1074/jbc.M111.228510.

99. Ohkuni,K. and Kitagawa,K. (2011) Endogenous transcription at the centromere facilitates centromere activity in budding yeast. *Curr. Biol.*, 10.1016/j.cub.2011.08.056.

100. Quénet,D. and Dalal,Y. (2014) A long non-coding RNA is required for targeting centromeric protein A to the human centromere. *Elife*, 10.7554/elife.03254.

101. Rošić,S., Köhler,F. and Erhardt,S. (2014) Repetitive centromeric satellite RNA is essential for kinetochore formation and cell division. *J. Cell Biol.*, 10.1083/jcb.201404097.

102. Catania,S., Pidoux,A.L. and Allshire,R.C. (2015) Sequence Features and Transcriptional Stalling within Centromere DNA Promote Establishment of CENP-A Chromatin. *PLoS Genet.*, 10.1371/journal.pgen.1004986.

103. Nye,J., Sturgill,D., Athwal,R. and Dalal,Y. (2018) HJURP antagonizes CENP-A mislocalization driven by the H3.3 chaperones HIRA and DAXX. *PLoS One*, 10.1371/journal.pone.0205948.
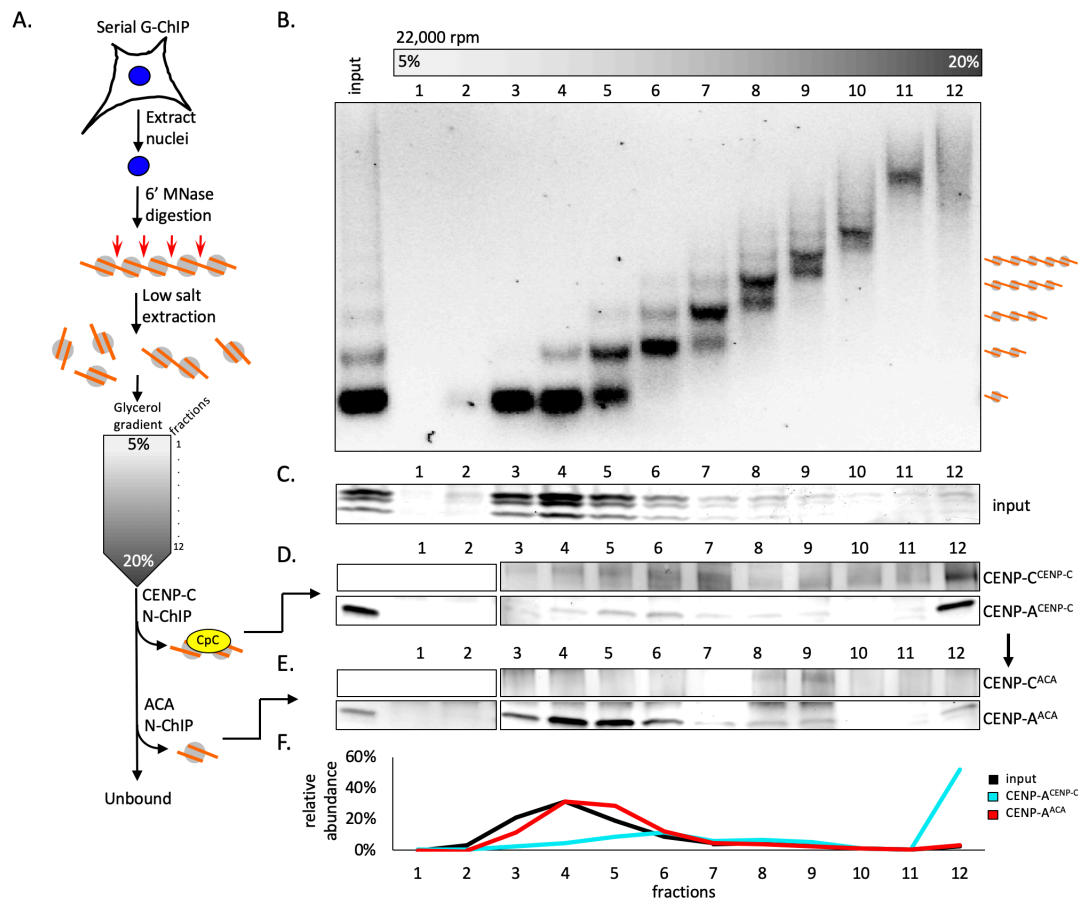
Figures

Figure 1

Figure 1. Two distinct classes of CENP-A nucleosome are found at the centromere

(A) Extracted chromatin was separated by a 5-20% glycerol gradient sedimentation assay from which twelve one mL fractions were isolated. (B) DNA from 50 μL aliquots per fraction was isolated and run on a 1.2% agarose gel. (C) Each fraction was run on a SDS-PAGE gel to determine the relative histone content. (D) Following CENP-C N-ChIP and (E) the subsequent serial ACA N-ChIP, each fraction was probed for CENP-C and CENP-A. (F) Quantification of relative histone levels from (C) or relative CENP-A from (D) and (E) levels per fraction. All experiments were performed in triplicates.
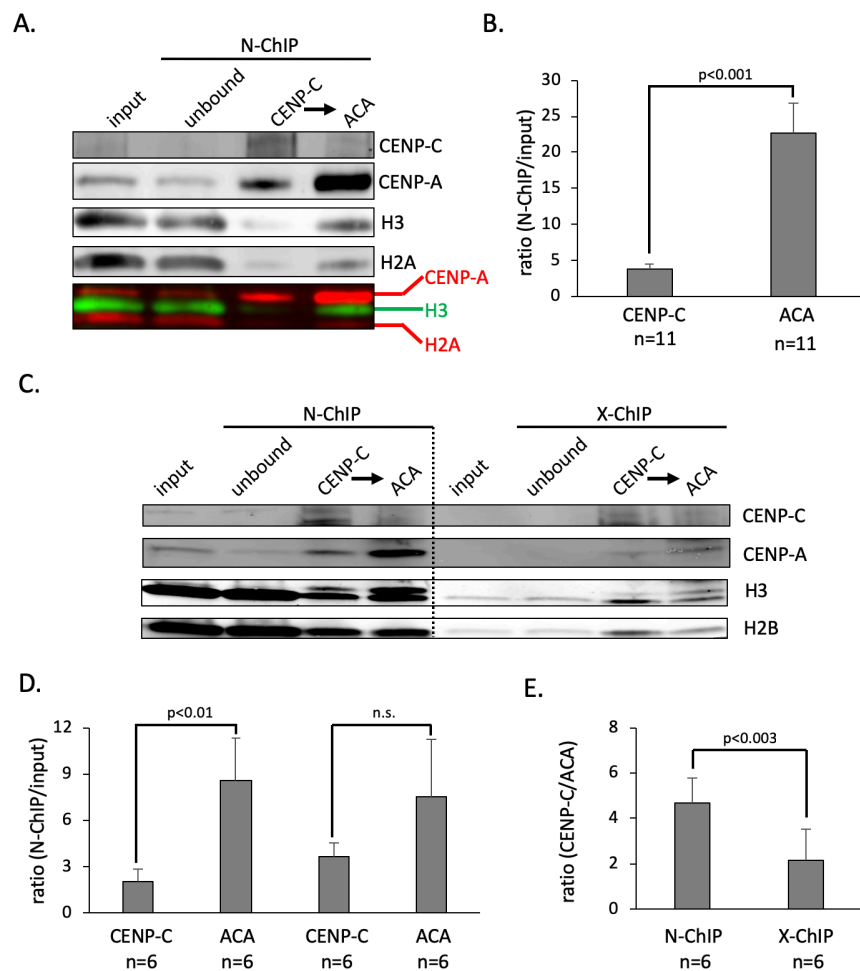
34

Figure 2

Figure 2. CENP-C binds CENP-A, not H3 nucleosomes

(A) Western blot analysis of the serial N-ChIP was performed and probed for H2A, H3, CENP-A, and CENP-C. (B) Quantification of eleven independent experiments revealed that a 6-fold difference between CENP-A bound to CENP-C and unbound CENP-A over input CENP-A levels (paired t-test $p<0.05$). (C) Western blot analysis comparing relative pull-down of both CENP-A population by either N-ChIP or X-ChIP. (D) Quantification of CENP-A enrichment in either CENP-C or subsequent ACA ChIP (paired t-test $p<0.05$). (E) Relative enrichment of CENP-A by ACA over CENP-C ChIP (2-sided t-test $p<0.05$).

35
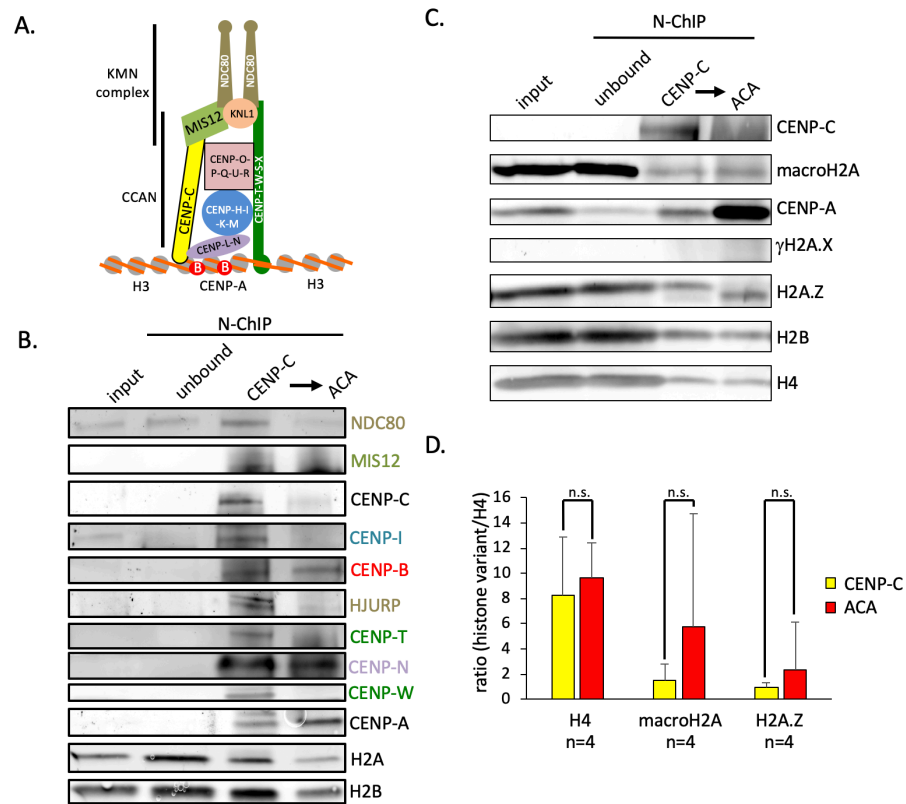
Figure 3

Figure 3. Small fraction of CENP-A associates with inner kinetochore

(A) To determine if CENP-C N-ChIP also brought down kinetochore components (B), chromatin

was extracted and ran on a SDS-PAGE, which was probed for the histones (H2A, H4, CENP-A),

CENP-B, inner kinetochore components (CENP-W, CENP-T, CENP-I, CENP-N), and outer

kinetochore components (MIS12, HEC1). (C) To determine whether histone H2A variants

associate with CENP-A nucleosomes in complex with CENP-C or bulk CENP-A, we performed

western blot analysis (B) probing for γH2A.X, H2A.Z, and macroH2A. (D) Quantification of

four independent experiments revealed that none of the H2A variants was enriched in either

CENP-A population. As a control, we measured the relative amount of H2B over H4 (paired t-

test $p < 0.05$).

Figure 4
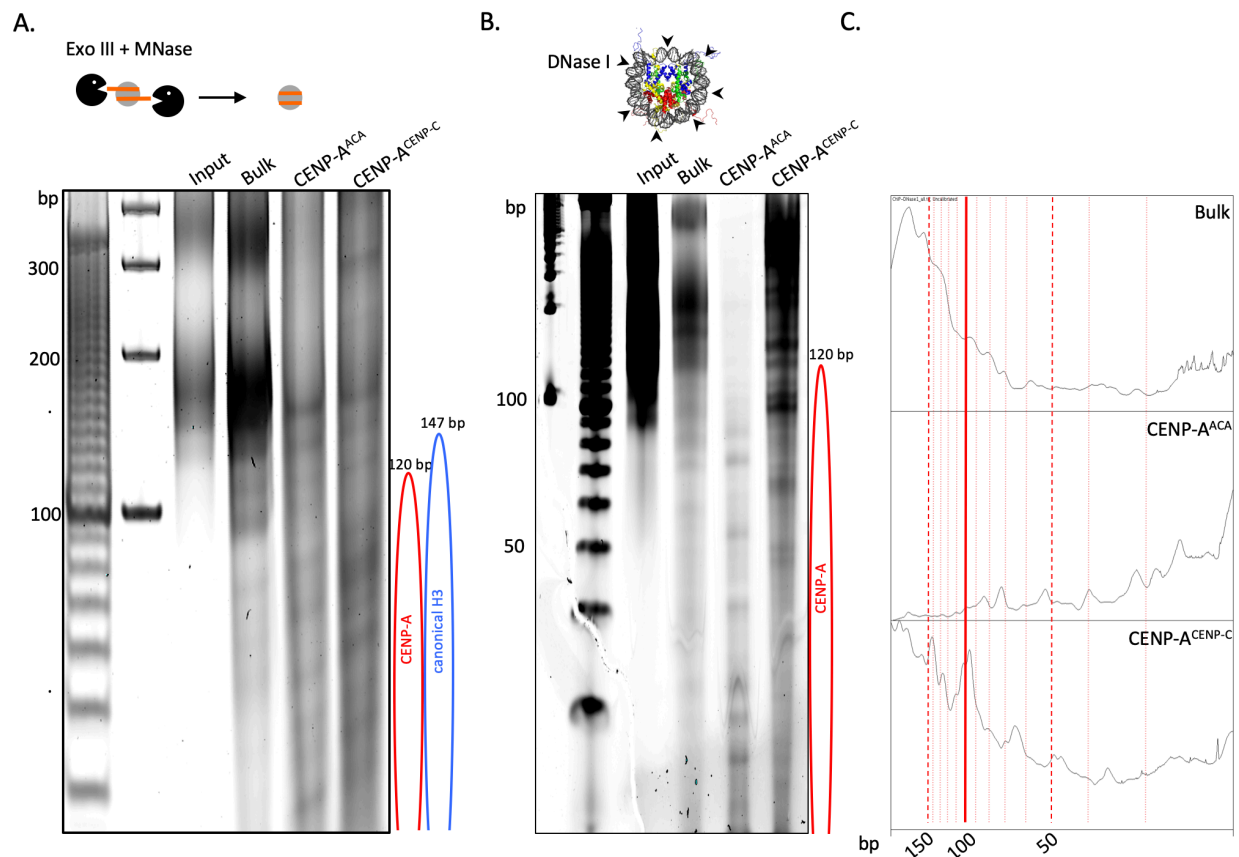
Figure 4. Inner kinetochore associated nucleosomes are not enriched for histone H2A variants

 (A) To determine how DNA is wrapped around nucleosomes, we isolated predominantly mononucleosomes following 15 minute MNase digestion of nuclei. Using Exonuclease III in combination with MNase the DNA entry and exit ends were digested. The resulting DNA products were resolved on 6% TBE gels. (B) Following DNase I digestion with 50 units of DNase I on ice for 50 minutes, DNA was extracted and ran on a 10% TBE with urea gel, allowing for separation of short DNA fragments. (C) A density plot of high resolution urea TBE gel.

Figure 5
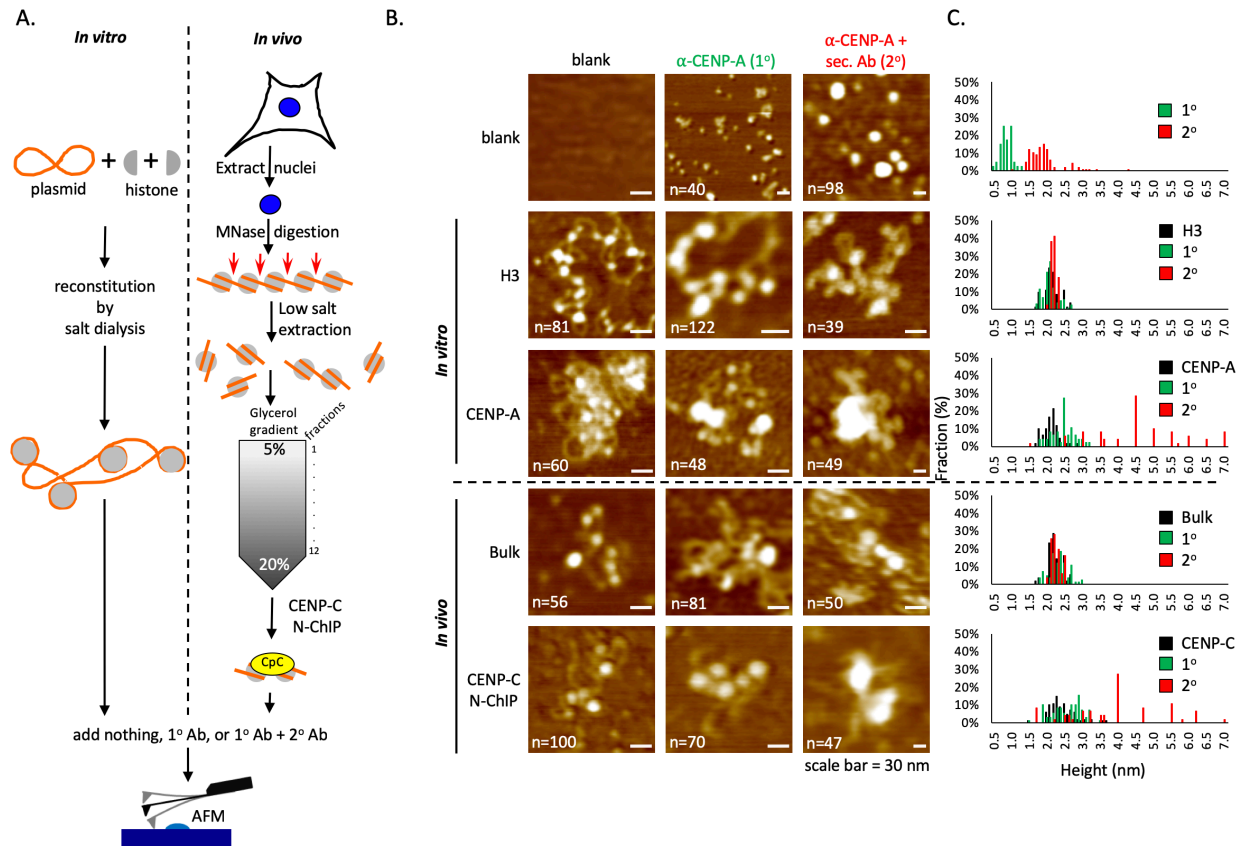
Figure 5. Immuno-AFM confirms CENP-C associates with CENP-A nucleosomes

(A) To confirm that CENP-C associated with CENP-A nucleosomes particles, we performed immuno-AFM on *in vitro* reconstituting H3 and CENP-A nucleosomes in parallel to extracted bulk and CENP-C associated chromatin. (B) Representative images for three conditions per sample, including a blank control. The scale bar is 30 nm. (C) Height measurement of all three conditions were plotted per sample, showing that anti-CENP-A antibody only recognized *in vitro* reconstituted CENP-A nucleosomes and nucleosomes associated with CENP-C.

Figure 6

scale bar = 50 nm
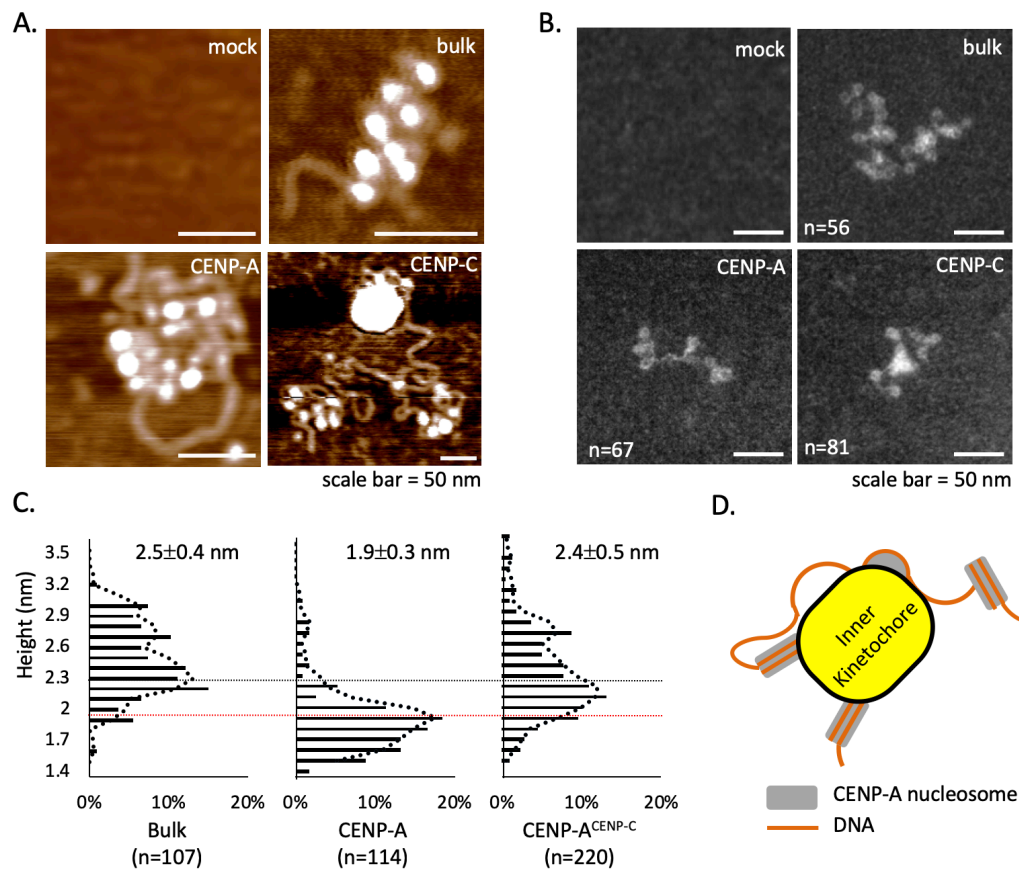
Figure 6. CENP-C complex associated with stable octameric CENP-A nucleosomes

(A) Chromatin was extracted from HeLa cells after 6-minute digestion, followed by either mock, CENP-A, or CENP-C N-ChIP. Unbound chromatin was used as bulk chromatin. Representative AFM (B) and TEM (C) images of either mock, bulk chromatin, CENP-A chromatin, or CENP-C chromatin. (D) Nucleosomal height was quantified for either bulk chromatin, CENP-A, or CENP-A nucleosomes associated with CENP-C complex. The mean height with standard error are shown, as well as their distribution. Robustly kinetochore associated CENP-A nucleosomes were significantly taller than weakly or not bound CENP-A nucleosomes (2-sided t test $p<2.6\cdot10^{-18}$). (E) A model showing how 4-6 CENP-A nucleosomes associate with the inner kinetochore, including a stretch of 230-bp of naked DNA that is refractory to MNase digestion.

Supplemental Figures

Supplemental Figure S1
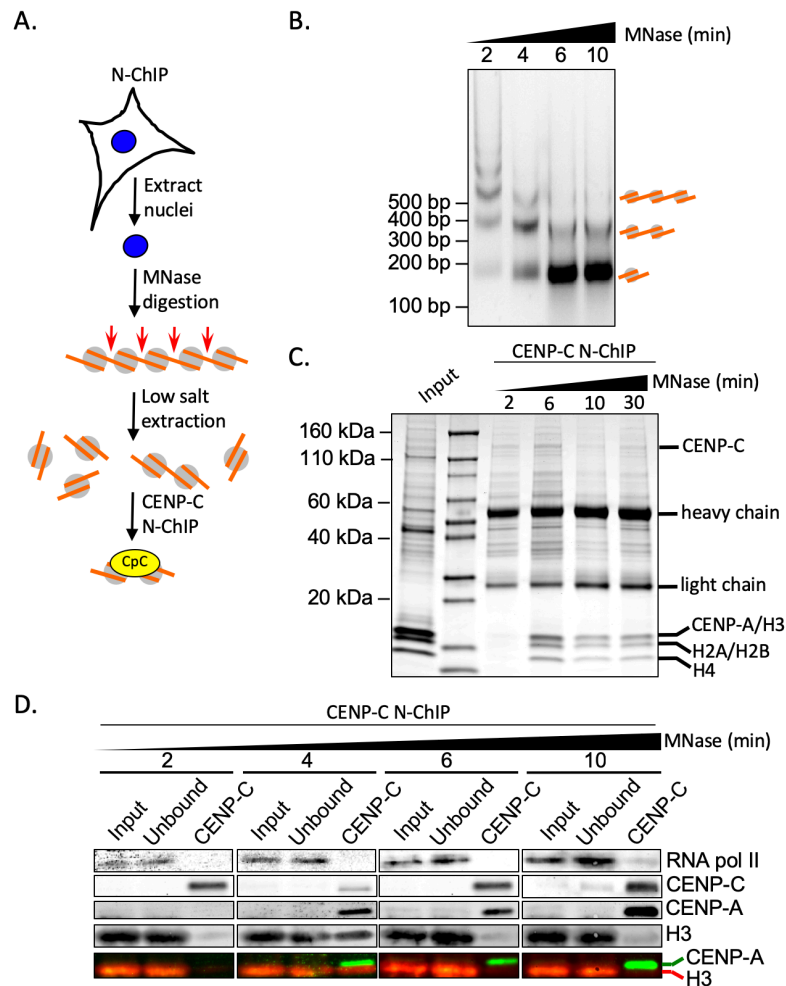
Figure S1. Six minute MNase digest ideal condition for isolating pure CENP-C:CENP-A complexes

(A) Experimental diagram how CENP-C associated chromatin was obtained. (B) DNA ladder followed a time course of MNase digestion, resolved on a 1% agarose gel. (C) CENP-C N-ChIP samples were resolved on 4-20% SDS Page and stained with SimplyBlue SafeStain. (D) Western blot analysis of CENP-C ChIP following a MNase time course, showing that after 6 minute MNase digestion, CENP-C ChIP almost exclusively pulls down CENP-A nucleosomes.

Supplemental Figure S2
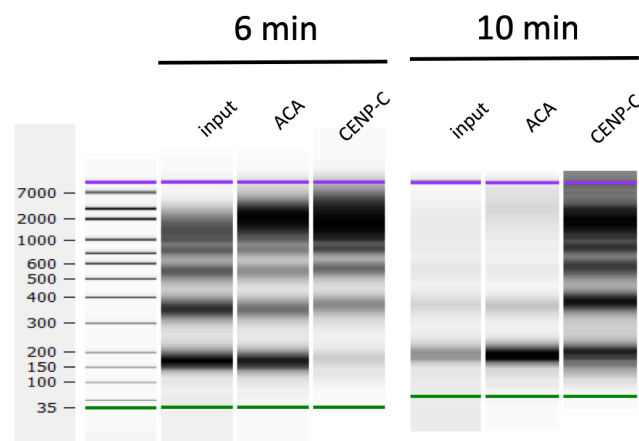
Figure S2. CENP-C associated chromatin is more refractory to MNase digestion than ACA chromatin

Chromatin from HeLa cells was digested with MNase for either 6 or 10 minutes and analyzed on the BioAnalyzer. CENP-C associated chromatin showed greater MNase digestion compared to bulk or ACA chromatin.

Supplemental Figure S3

A.

B.

Monomers	ACA		CENP-C	
	Count	Fraction	Count	Fraction
ALR	35	3.12%	6	2.80%
ALR1	60	5.35%	10	4.67%
ALR2	17	1.52%	12	5.61%
Hasson	457	40.77%	90	42.06%
Henikoff_Cen1	454	40.50%	76	35.51%
Henikoff_Cen13	98	8.74%	20	9.35%
Total	1121	100.00%	214	100.00%
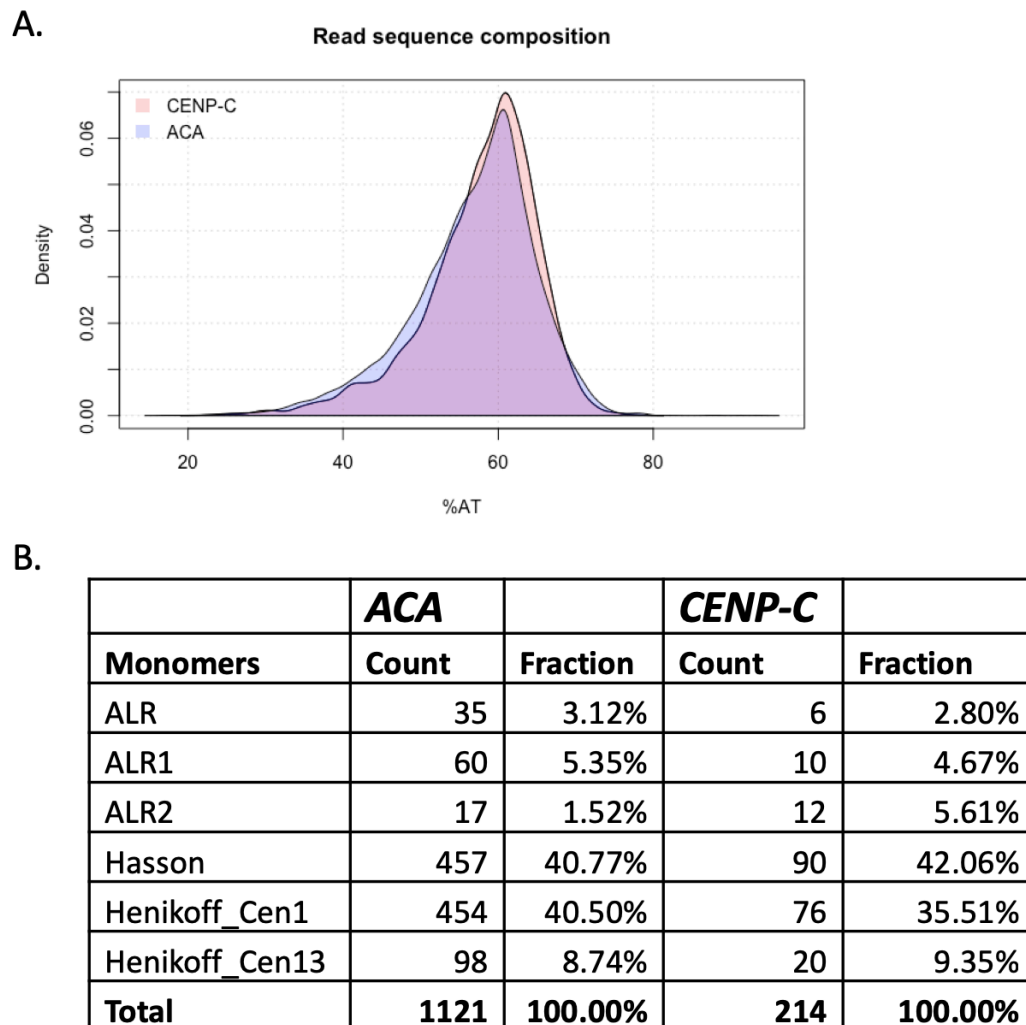
Figure S3. Both CENP-A populations occupy essentially the same

The obtained PacBio sequence reads from either CENP-C and subsequent ACA N-ChIP were

compared for their AT content as a first estimate if they might occupy different sequences.

Second, the sequence reads were aligned to established centromeric α-satellite sequences. In

both cases no differences were observed. ALR, ALR1, and ALR2 are α-satellite DNA from

RepBase, Hasson is baed on the sequence used by Hasson et al 2013, Henikoff_Cen1 and

Henikoff_Cen13 were derived from Henikoff et al 2015.

Supplemental Figure S4
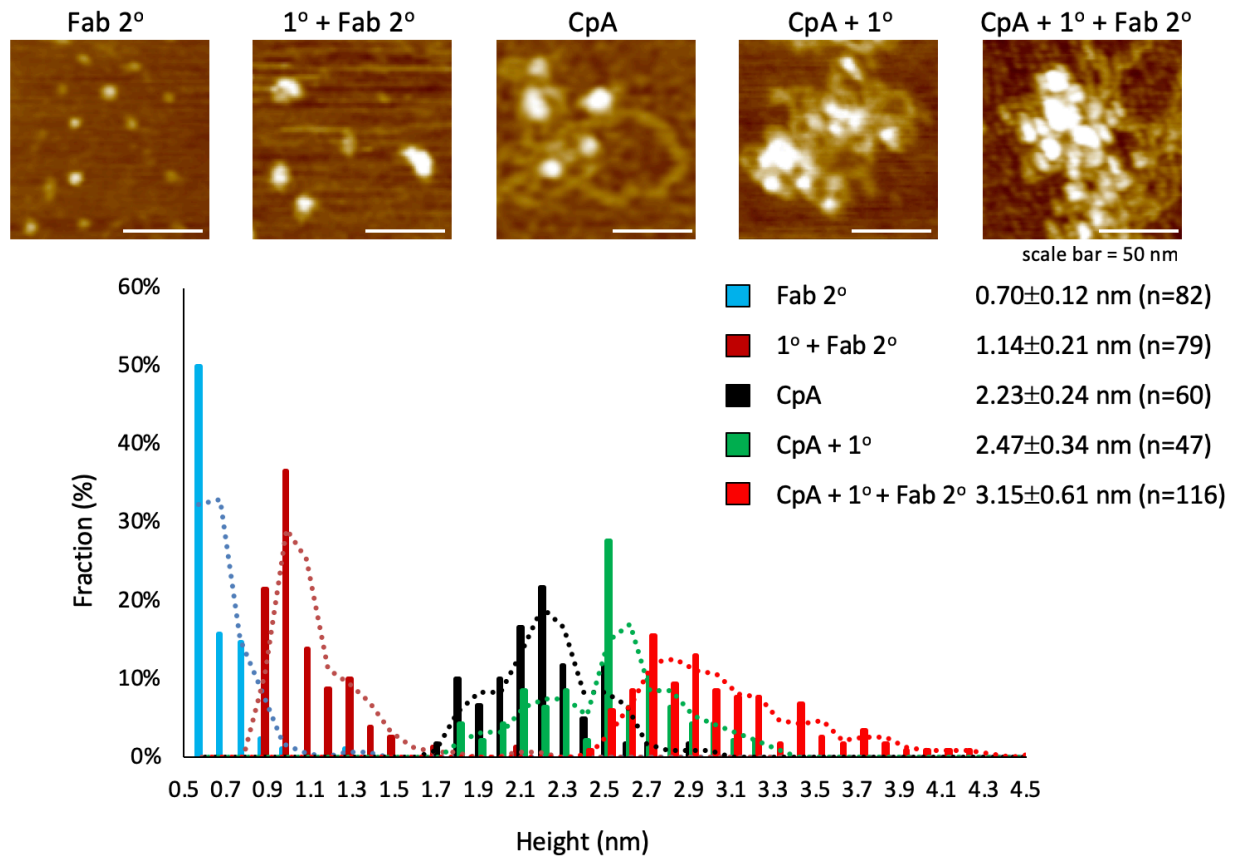
Figure S4. Immuno-AFM confirms CENP-A nucleosome identity by Fab fragment.

To confirm that the secondary antibodies used in Figure 5 did not result in aberrant confirmation due to clustering induced by the secondary antibodies, we also confirmed CENP-A nucleosome identity using the anti-mouse Fab fragment.

Supplemental Figure S5
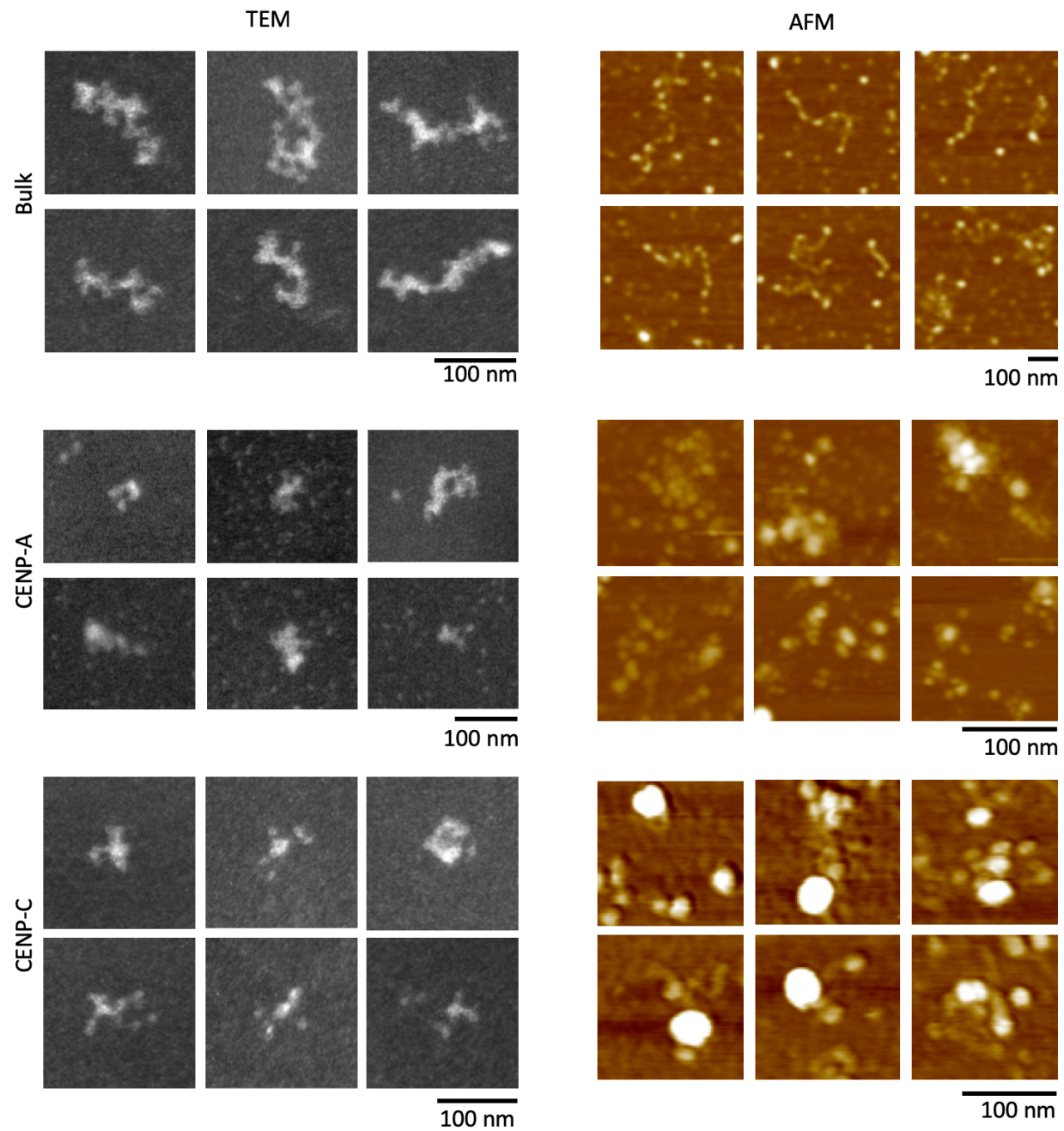
Figure S5. Representative TEM and AFM images of bulk, CENP-A, and CENP-C chromatin

For each condition, six representative images are shown. The scale bar is 100 nm.

Supplemental Tables

Table S1. Quantification of CENP-A levels for the two CENP-A populations

From HeLa cells, native centromeric chromatin was isolated by serial CENP-C and ACA N-ChIP. CENP-A levels were quantified from Western blot. 6-11 independent replicates were quantified using LiCor software. Quantification of CENP-C or ACA over input demonstrated that under native ChIP conditions, 6-fold excess of weakly bound CENP-A exist over robustly bound CENP-A, whereas under cross-linked ChIP conditions, an almost two-fold excess was found. Overall, these analyses confirm that two dinstinct and sizable CENP-A populations exist in cycling human cells. Values are a.u.

| Table S1: a sizable fraction of CENP-A chromatin is not strongly associated with CENP-C						
N-ChIP quantification for Figure 2B						
	input	CENP-C IP	ACA IP	CENP-C/input	ACA/input	ACA/CENP-C
Exp1.1	0.609	4.45	23.4	7.31	38.42	5.26
Exp1.2	0.609	4.81	25.4	7.90	41.71	5.28
Exp1.3	0.543	2.3	11.4	4.24	20.99	4.96
Exp1.4	0.317	1.43	9.46	4.51	29.84	6.62
Exp1.5	0.463	1.64	13	3.54	28.08	7.93
Exp1.6	0.431	4.33	37.3	10.05	86.54	8.61
Exp1.7	1.88	5.85	36.1	3.11	19.20	6.17
Exp1.8	1.88	3.87	48.8	2.06	25.96	12.61
Exp1.9	1.88	6.4	32.7	3.40	17.39	5.11
Exp1.10	26.2	41.7	86.9	1.59	3.32	2.08
Exp1.11	26.2	24.5	67.3	0.94	2.57	2.75

	CENP-C/input	ACA/input	ACA/CENP-C
mean	4.42	28.55	6.12
median	3.54	25.96	6.12
stdev	2.85	22.85	2.89
SE	0.86	6.89	0.87
Paired t test		0.001	

N-ChIP quantification for Figures 2D, E						
	input	CENP-C IP	ACA IP	CENP-C/input	ACA/input	ACA/CENP-C
Exp2.1	0.912	2.3	14.7	2.52	16.12	6.39
Exp2.2	0.561	3.34	10	5.95	17.83	2.99
Exp2.3	26.6	13.4	57.8	0.50	2.17	4.31
Exp2.4	26	15.2	81.3	0.58	3.13	5.35
Exp2.5	7	9.76	43.8	1.39	6.26	4.49
Exp2.6	9.07	11.8	52.3	1.30	5.77	4.43

X-ChIP quantification for Figures 2D, E						
	input	CENP-C IP	ACA IP	CENP-C/input	ACA/input	ACA/CENP-C
Exp3.1	7.5	31.4	42.8	4.19	5.71	1.36
Exp3.2	6.98	23.3	21.7	3.34	3.11	0.93
Exp3.3	7.71	0.86	3.37	0.11	0.44	3.92
Exp3.4	3.44	9.66	17.6	2.81	5.12	1.82
Exp3.5	1.44	7.18	7.41	4.99	5.15	1.03
Exp3.6	0.31	2.05	7.96	6.61	25.68	3.88

	N-ChIP		X-ChIP			ACA/CENP-C	
	CENP-C/input	ACA/input	CENP-C/input	ACA/input		N-ChIP	X-ChIP
mean	2.04	8.54	3.67	7.53	mean	4.66	2.16
median	1.35	6.01	3.76	5.13	median	4.46	1.59
stdev	2.05	6.73	2.20	9.10	stdev	1.14	1.39
SE	0.84	2.75	0.90	3.71	SE	0.46	0.57
Paired t test		0.012		0.132	Two-sided t test		0.003

Table S2. Quantification of histone H2A variants levels for the two CENP-A populations
From HeLa cells, native centromeric chromatin was isolated by serial CENP-C and ACA N-ChIP. CENP-A levels were quantified from Western blot. 4 independent replicates were quantified using LiCor software. Quantification of H2B, macroH2A, and H2A.Z over H4 demonstrated that under native ChIP conditions, no significant enrichment was observed between either CENP-C or the serial ACA N-ChIP.

Table S2. Histone H2A variants are not relatively enriched in either CENP-A population								
	CENP-C IP				ACA IP			
	H4	macroH2A	H2AZ	H2B	H4	macroH2A	H2AZ	H2B
Exp1	2.9	2.43	3.58	30.1	2.35	1.76	2.59	23.2
Exp2	1.43	2.21	2.07	29.7	1.69	1.45	3.04	22.3
Exp3	2.47	2.92	0.83	1.67	0.136	5.19	2.34	1.99
Exp4	0.512	3.27	0.99	1.07	0.595	14.4	2.73	1.53

mean	1.83	2.71	1.87	15.64	1.19	5.7	2.68	12.26
median	1.95	2.68	1.53	15.69	1.14	3.48	2.66	12.15
stdev	1.07	0.48	1.27	16.47	1.01	6.04	0.29	12.13
SE	0.54	0.24	0.63	8.24	0.51	3.02	0.015	6.06

	Ratio histone variant over H4						
	CENP-C				ACA		
	macroH2A/H4	H2AZH4	H2B/H4		macroH2A/H4	H2AZH4	H2B/H4
Exp1	0.84	1.23	10.38		0.75	1.10	9.87
Exp2	1.55	1.45	20.77		0.86	1.80	13.20
Exp3	1.18	0.34	0.68		38.16	17.21	14.63
Exp4	6.39	1.93	2.09		24.20	4.59	2.57

mean	9.95	4.95	33.91		63.97	24.70	40.27
median	1.36	1.34	6.23		12.53	3.19	11.53
stdev	2.62	0.67	9.24		18.44	7.51	5.38
SE	1.31	0.33	4.62		9.22	3.75	2.69
Paired t test					0.114	0.154	0.374

Table S3. Quantification of immuno-AFM measurments

In order to assess whether CENP-C would associate with CENP-A nucleosomes, immuno-AFM was used on both in vitro reconstituted H3 and CENP-A nucleosomes, as well as bulk chromatin and CENP-C ChIP'ed chromatin from HeLa cells. In vitro reconstituted H3 nucleosomes did not change in height upon exposure to anti-CENP-A antibody or the combination of anti-CENP-A + anti-mouse secondary antibody. In contrast, CENP-A nucleosomes did change height substantially (Figure 5). Using an anti-mouse Fab fragment also showed a change in height of CENP-A nucleosomes (Figure S4). Finally, bulk chromatin was purified from HeLa cells, but did not show change in nucleosome height upon exposure to either anti-CENP-A antibody or anti-CENP-A antibody + anti-mouse secondary antibody. Nucleosomes associated with the CENP-C complex did, thereby confirming the identity of the associated nucleosomes as CENP-A nucleosomes.

Table S3. Quantification of immuno-AFM to identify CENP-A nucleosomes										
					In vitro reconstituted nucleosomes					
					H3 nucleosome			CENP-A nucleosome		
1 antibody	X	X		X		X	X		X	X	X
2 antiobdy		X					X			X	
2 Fab			X	X							X
N	40	99	82	79	81	122	37	60	48	49	120
mean (nm)	0.9	2	0.7	1.1	2.2	2.1	2.2	2.2	2.5	4.6	3.2
stdev	0.2	0.5	0.1	0.2	0.2	0.2	0.1	0.2	0.3	1.4	0.6

					In vivo purified chromatin					
					bulk chromatin			CENP-C chromatin		
1 antibody						X	X		X	X
2 antiobdy							X			X
2 Fab										
N					56	81	50	100	70	49
mean (nm)					2.3	2.4	2.3	2.4	2.6	3.9
stdev					0.2	0.3	0.1	0.4	0.4	1.3

48

Table S4. Quantification of CENP-C complex dimensions and refractory naked DNA.
CENP-C chromatin was isolated from HeLa cells and imaged by in air AFM by non-contact tapping mode. The height and surface area dimensions were obtained. In addition, frequently a DNA loop was observed coming out of the CENP-C complex. By ImageJ these strechtes of DNA were measured.

Table S4. CENP-C complex dimensions and associated DNA loop		
CENP-C complex dimensions		
mean height (nm)	5.57	N=177
median height (nm)	4.95	
stdev	2.05	
mean area (nm^2)	629	N=177
median area (nm^2)	540	
stdev	358	
Length of naked DNA loop		
mean length (bp)	232.9	N=44
median length (bp)	148.5	
stdev	267.2	

Table S5. CENP-C associated CENP-A nucleosomes have octameric dimensions.
From HeLa cells CENP-A and CENP-C chromatin were purified. The unbound fraction was used as bulk control. Chromatin was visualized by in air AFM in non-tapping contact mode. Nucleosomal height was determined by ImageJ as well as manual spot checking.

Table S5. Nucleosomal height of bulk, CENP-C associated CENP-A nucleosomes, and CENP-A nucleosomes			
	In vivo extracted chromatin		
	bulk	CENP-A	CENP-C
N	107	114	220
mean height (nm)	2.5	1.9	2.4
median height (nm)	2.5	1.9	2.3
stdev	0.3	0.3	0.45
SE	0.03	0.03	0.03
Two-sided t test			2.64E-18